RESTRAINED SHRINKAGE BEHAVIOR OF CRIMPED STEEL FIBER REINFORCED SELF-CONSOLIDATING CONCRETE

By

GIUSEPPE LIBERTI

A thesis submitted to the

Graduate School – New Brunswick

Rutgers, The State University of New Jersey

In Partial Fulfillment of the requirements

For the degree of

Master of Science

Graduate Program in Civil & Environmental Engineering

Written under the direction of

Dr. Hani H. Nassif

And Approved by

_____

_____

_____

New Brunswick, New Jersey

May 2017

ABSTRACT OF THE THESIS

RESTRAINED SHRINKAGE BEHAVIOR OF CRIMPED STEEL FIBER REINFORCED SELF-CONSOLIDATING CONCRETE

By GIUSEPPE LIBERTI

Thesis Director:

Dr. Hani Nassif

The use of self-consolidating concrete (SCC) is becoming more popular thanks to its superior workability and its ability to consolidate under its own weight without the need for external compaction or vibration. With the advancements of admixtures like superplasticizers, SCC can now match the strength and other properties similar to high performance concrete (HPC). SCC contains a higher amount of cementitious material than ordinary HPC which makes it prone to higher levels of shrinkage which can be problematic in situations where the concrete is restrained. When concrete is restrained, shrinkage induced cracking can occur.

This study compares the restrained shrinkage properties of an SCC mix controlled with 1½ in. crimped steel fibers mixed in. The SCC control mix without fiber is compared with mixes containing 0.35, 0.50, 0.65, and 0.80% of steel fiber by volume. To improve workability, additional superplasticizer, in the form of high range water reducer (HRWR), was added accordingly. Mixes above 0.65% by volume did not pass the fresh properties and workability requirements even with the additional HRWR. Strength was

shown to decrease with the addition of fibers, sometimes up to 40%, but regained strength at higher fiber contents. Free shrinkage was also monitored but shown to have minimal effects. To understand the restrained shrinkage behavior of the mixes, one ASTM restrained shrinkage ring in accordance with ASTM C 1581 and two AASHTO restrained shrinkage rings in accordance with ASTM T334 were casted for each mix. The AASHTO T334 ring was modified to place 6 vibrating wire strain gauges (VWSG) to directly measure the strain in the concrete and predict where cracks will form. Despite the lower strength, the FRSCC mixes delayed and sometimes prevented large cracks from forming and propagating, reduced crack widths up to 73%, and reduced total cracking area by up to 73% compared the control mix. Between the two ring tests, the ASTM ring induced larger cracks earlier than the AASHTO ring making for easier and quicker results.

ACKNOWLEDGEMENTS

I would first like to thank Dr. Hani Nassif for his support throughout all my undergraduate and graduate studies at Rutgers. Dr. Nassif inspired me to challenge myself intellectually and gave me the opportunity to prove myself as an undergraduate research assistant since my sophomore year. It has been an honor for me to work with him not only as my advisor but as a mentor for me to look up to.

I would like to thank Dr. Najm and Dr. Wang for being on my committee, as well as being great teachers as both an undergraduate and graduate student here at Rutgers.

I would also like to thank Adi Ab-Obeidah for his amazing support in Civil Engineering Lab. Since starting as an undergraduate research assistant, Adi has always been there to offer support, advice, and motivation to be the best I can. He helped me overcome many problems and was an amazing colleague to work with.

I would like to thank the undergraduate and graduate research assistants who assisted me in this endeavor including Dalexander Gonzales, Zaina Hamdan, Mirelle Alktaish, Christopher Sholy, Elie Haddad, and Gregory Brewer, for the countless hours of mixing, testing and crack-mapping. Although the work was tiring and relentless at times, they helped out and without their help this work would have been impossible. I would also like to thank my family and close friends for their endless love and support.

I would like to thank Euclid Chemical, LaFargeHolcim, and Clayton Concrete for their generous donation of materials towards the completion of this study. Finally, I would like to thank the RE-CAST University Transportation Center for funding my research as well as the Rutgers Civil & Environmental Engineering department.

Table of Contents

LIST OF TABLES

LIST OF FIGURES

CHAPTER I

1 INTRODUCTION

1.1 Problem Statement

Concrete is the most widely used construction material due to its versatility and relatively low cost. Concrete can be poured like a liquid and takes the shape of whatever it is poured into and hardens into a structural building material. In the transformation to its solid form, concrete naturally loses some of its volume in a phenomenon known as shrinkage. Shrinkage can lead to a host of problems, very notably when concrete is restrained. Restrained conditions physically prevent the concrete from undergoing the change in volume. This allows stresses to build up and can lead to shrinkage cracking. Once a crack forms, it is easy for a crack to propagate and become larger and wider. This can happen due to loading, freeze-thaw, temperature changes, and deicing salts. These large cracks allow water and chemicals to reach the embedded steel rebars and promote corrosion. The corrosion and rust widens cracks even further providing a positive feedback mechanism to increased corrosion leading to expensive bridge deck replacements.

Shrinkage alone does not generally lead to cracking, but a combination of high shrinkage with low tensile strength, low cracking resistance, and restrained conditions can cause cracking to happen. Restrained conditions can come from a variety of sources such as embedded rebar, shear studs, steel girders, cold joints, etc. These conditions occur more often in bridge decks near abutments and in the negative moment regions. Restrained

conditions are sometimes unavoidable so it is important to choose a concrete that has a higher tensile strength, higher cracking resistance, and lower shrinkage to prevent cracking and/or resist cracks from propagating.

In an effort to save labor costs, time, and provide better workability, the construction industry has began to utilize Self-Consolidating Concrete (SCC) for their concrete mixes. SCC refers to a group of highly workable concrete that can fill tight voids and spaces without the need for external compaction or vibration. SCC keeps a low viscosity without segregation or bleeding which makes it very valuable when space is tight in cases where there is tight rebar spacing or in repair. SCC's value also comes in the reduced labor and equipment needed since you don't need a crew or vibrators to compact the concrete when placed.

Self Consolidating Concrete typically requires a higher water content and paste volume to achieve its workability properties. This sometimes leaves SCC prone to higher shrinkage than HPC and other types of concrete used on bridge decks. All aspects of a concrete mix have a role in the strength and shrinkage behavior. By studying the ratios and balances of cementitious material, aggregate, water, and chemical admixtures a low shrinkage, high strength SCC mix can be designed.

Fibers are sometimes added to concrete mixes to increase tensile strength and provide cracking resistance. Typical fiber materials used are steel, polypropylene, and polyvinyl-alcohol (PVA). SCC mixes with fiber are referred to as Fiber Reinforced Self-Consolidating Concrete (FRSCC). The amount of fiber used in SCC must be closely monitored in order to insure clumping, segregation, and bleeding does occur and

workability remains high enough to be considered SCC. FRSCC combines the benefits of SCC with the added cracking resistance of fibers and can be a great, profitable option for bridge decks and other structures.

1.2 Research Objectives and Scope

The purpose of this research is to compare the restrained shrinkage properties and performance of self consolidating concrete with crimped steel fibers of varying amounts. The steel fibers used are 1 1/2" long and crimped shape to help the concrete bond to it and provide better cracking resistance without too much effect on the slump flow. Fibers will be added by percent by volume of 0.00%, 0.35%, 0.50%, and 0.65%. The SCC mix will have a water to cement ratio of .425 with a total cementitious content of 675lb/cu yd. Portland Type I cement will be used with 35% being substituted with grade 120 slag to provide greater strength. The aggregate used will be equal amounts of #8 coarse aggregate and fine aggregate (sand). Air entraining and water reducing admixtures will be used to achieve desired slump and air contents. The fresh properties of the mixes will be analyzed for slump flow, workability, and quality assurance. The mechanical properties including compression, tension, and modulus of elasticity will be taken for all mixes. The shrinkage properties will be evaluated via free shrinkage tests and restrained shrinkage tests using both ASTM rings and AASHTO rings.

CHAPTER II

2 LITERATURE REVIEW

2.1 Types of Shrinkage

Shrinkage occurs at every stage of concrete's life from the instant it is casted through its entirety of life. The rate and extent of shrinkage is dependent on the characteristics and proportions of the mix. There are different types of shrinkage including plastic shrinkage, thermal shrinkage, autogenous shrinkage and drying shrinkage and each affects the concrete in different ways depending on age and outside factors.

2.1.1 Plastic Shrinkage

Plastic shrinkage occurs within a couple hours after mixing. The concrete is in a plastic state during this time and has not gained its strength. When unrestrained, the concrete can freely shrink as it loses some volume. If restrained, plastic shrinkage can lead to cracking as tensile stresses can build up. The majority of the loss in volume comes from the evaporation of the water within the concrete. This can be accelerated when in hot, dry, and windy weather conditions (Mora-Ruacho et al, 2009). Fogging and wet curing can help to eliminate plastic shrinkage especially if it is done before the concrete begins to harden.

Different admixtures can have an effect on the hydration process and the rate of evaporation. In a study by Leeman, Nygaard and Lura, accelerators were found to decrease bleeding settlement and capillary pressure leading to earlier cracking, while retarders helped retain moisture at the surface and reduce plastic shrinkage (Leeman,

Nygaard, and Lura, 2009). Studies have shown that during the first few hours, fiber reinforced concrete behaves the same as plain concrete and so the factors affecting the plastic shrinkage of plain concrete will also pertain to fiber reinforced concrete (Wongtanakitcharoen and Naaman, 2007).

2.1.2 Thermal Shrinkage

As with any material, concrete expands and contracts as a result of thermal expansion and contraction of the concrete. Thermal shrinkage is dependent on both temperature and the coefficient of thermal expansion (CTE). Temperatures rise and fall constantly throughout the day, so concrete exposed to the outdoors constantly undergo cycles of thermal stress. Large variations in temperature and wind induce large thermal stresses.

The CTE in concrete varies based on the different components of the concrete. Issues arise during the exothermic hydration reaction during the curing of concrete. As soon as water touches the cement, the temperature of the concrete steeply rises. When the reaction slows, temperature begins to cool and the concrete contracts due to thermal shrinkage. Type II cement reduces thermal stresses and pozzolans both can reduce the rate of hydration and lowers the heat produced during hydration. Higher aggregate to paste ratios tend to have a lower CTE (Deng 2016). Water content and distribution of pores also play a large role in controlling the coefficient. When concrete has many pores for water to enter, the water can reach equilibrium quicker and the shrinkage is not as severe (Sellevold and Bjøntegaard, 2006).

2.1.3 Autogenous Shrinkage

Autogenous shrinkage is the change in volume of concrete as a result of the hydration process of cement. Unlike thermal shrinkage, where the volume loss is due to the cooling after the steep rise in temperature during the early hydration, autogenous shrinkage is a result of the cement particle creating a fine network of pores throughout the concrete as a result of hydration. The hydrating cement drains water from course capillaries formed from the mixing of the concrete. If there is no external source of water, such as bleeding or wet curing, the outer capillaries are drained and experience drying. This is known as self-desiccation (Barcelo, Moranville, & Clavaud 2005).

One of the largest factors of autogenous shrinkage is the water to cement ratio. A lower water to cement ratio increases autogenous shrinkage and shrinkage begins earlier. Finer cement particles also increase autogenous shrinkage (Tazawa 1995). The use of pozzolans such as slag has been shown to reduce early age autogenous shrinkage but higher or similar long term shrinkage compared to solely cement (Wei et al. 2011). In the past, autogenous shrinkage was negligible or very small as most concrete mixes had high water to cement ratios. However with the advancements in chemical admixtures and cement manufacturing, mixes of today tend to have lower water to cement ratios so autogenous shrinkage is becoming a larger problem.

2.1.4 Drying Shrinkage

Drying Shrinkage is similar to autogenous shrinkage and is sometimes classified as the same. Drying shrinkage refers to the evaporation of water from the concrete, but has nothing to do with the hydration process. Both types of shrinkage reduce the pore relative humidity which evidently leads to the change in volume as water is either used up or

evaporated. Drying shrinkage is the longest process of shrinkage and continues beyond a year. The time dependence of drying shrinkage is dependent on the material properties, size, and environment.

The rate of drying is very quick at first but slows over time. Over time, pore water moves towards the surface through a complex pore network. Drying occurs from the surface and inwards. Structures with a large surface area will experience more shrinkage than a large structure with not a lot of surface area. On bridge decks, drying is large as it is exposed to the air and surface area to volume ratio is quite large.

The porosity plays a large role in the rate of drying. A decrease in pore size with a large percentage of small sized pores increases shrinkage. This can be explained by the decrease in crystallinity (Narayanan & Ramamurthy, 2000). When steel fibers are added, porosity rises and the rate of drying increases (Jafarifar et al. 2014).

2.2 Self Consolidating Concrete

Self Consolidating Concrete, sometimes referred to as Self Compacting Concrete (SCC), is a relatively new class of concrete with excellent workability and segregation resistance developed in the 1980's in Japan (Ahmad et al. 2014). SCC has the ability to fill gaps of reinforcement and corners of molds without the need for vibration and compaction unlike HPC. HPC mix designs emphasize strength and durability, but have just enough workability to be placed with the need for vibration and compaction (Su et al. 2001). The properties of SCC make it a viable economic alternative to HPC or conventional vibratable concrete (CVC). Contractors and the precast industry can save money by reducing labor costs, eliminating the need for vibrating equipment, and accelerated

pouring times. Although the raw materials of SCC may be slightly higher, the overall profitability can be upwards of 10% (Szecsy, 2002). SCC is also better for the environment and for the people working with it. Noise levels have been observed to be reduced about 25%. Energy consumption can be reduced about 62% depending on the project, and CO_2 emissions can be lowered due to the changes in amount of cement needed and use of pozzolans (Bier & Rizwan, 2014).

There are several definitions of SCC but there is consensus that the mixture should flow and fill the forms under its own weight without vibration, it should remain homogeneous regardless of distance it flows, and it can flow through congested reinforcement and confined spaces without losing its filling ability characteristics (Bonen & Shah, 2004). To ensure a concrete mix design meets these definitions, standard testing procedures have been developed. The slump flow test measures the free flow ability. There are no guidelines set but SCC will generally slump over 20 inches in under 8 seconds. To check its filling properties and segregation resistance, a J ring test can be performed. Made to replicate tightly spaced rebar, the J ring test ensures that the concrete can flow with little impediment and resistance to segregation by visual inspection. There is a drive for research in the materials and admixtures to help maintain these characteristics, while making a strong, durable SCC mix design.

There are three common characteristics among most SCC mixes; a limited aggregate content, low water to powder ratio (W/P), and the use of superplasticizer. Large amount of aggregate causes friction and takes away the energy that helps SCC flow. When the W/P ratio and superplasticizer dosage are held constant, both the mechanical properties and the flow of SCC decreases as aggregate size increases (Khaleel et al. 2011). It is

recommended to use less amounts of small, well graded, rounder aggregate. A low (W/P) ratio can be achieved by substituting cement with pozzolans such as slag, fly ash, or silica fume. In general, an increase in slag content increases workability but can lead to bleeding and segregation at high amounts (Boukendakdji et al. 2009). The use of plasticizers has revolutionized concrete as it can increase the workability of concrete without the need for additional water and are a vital component in SCC.

Superplasticizers, or high-range water reducers (HRWR), are a chemical admixture meant to add more slump to a concrete mix. They work by binding to the cement particles and preventing them from clumping together due to their electric charge (Pumphrey, 2012). The amount and type of HRWR used can vary from mix to mix and can be adjusted to achieve the desired slump and workability. The setting time and application all play a role in choosing the right type of superplasticizer. The precast industry, where the concrete is casted in only 10-30 minutes, may prefer to use an acrylic copolymer based HRWR since it has a short setting time but can achieve a high early strength. A ready mixed concrete may need four times longer before it is placed so adjusting the dosage of a Carboxylate-terpolymer or Polyoxyethylene copolymer based HRWR can delay the setting time up to 2 hours (Felekoğlu & Sarıkahya, 2008). In addition to superplasticizers, viscosity modifying admixtures (VMA) can also be added to achieve less segregation and bleeding when used in conjunction with superplasticizers (Lachemi et al. 2004). Superplasticizers and other admixtures provide some flexibility in a mix design and can help achieve desired slump, prevent bleeding, and extend setting time if chosen carefully with the correct dosage.

Another admixture that is sometimes added to concrete is an air entraining admixture (AEA). AEA is used when the concrete is in cold environments or susceptible to freeze-thaw such as dams, bridges, and tunnels. AEA allows microscopic bubbles to form while mixing. When trapped water freezes during cold temperatures, the water expands and takes up the space of the small air pockets. Without them, the water would exert a lot of pressure on the crystalline structure of the concrete and potentially form cracks. Freeze-thaw test results have indicated only a slight dependence on the type of HRWR but the biggest effect on the results was the addition of AEA to maintain its strength and crack resistance after many cycles of freeze thaw. In regards to flowability, AEA in smaller doses can increase slump diameter, while AEA in higher doses can decrease the flow due to the interaction of the air bubbles and concrete particles (Łaźniewska-Piekarczyk, 2012).

The benefits of SCC are quite clear but there are some problems with it. The higher cement content of SCC leaves it vulnerable to higher shrinkage than conventional concrete. If the concrete is restrained, the high shrinkage leads to higher strain. Cracking can occur if the strain exceeds the tensile stress in the concrete. To mitigate shrinkage, proper curing and shrinkage reducing admixtures can be used, but cracking potential will still be typically higher than conventional concrete (Loser & Leemann, 2009).

2.3 Fiber Reinforced Concrete

2.3.1 History of Fiber Reinforced Concrete

Concrete by nature is a very brittle material. To increase the ductility of materials, fibers are sometimes added. In the 1960s, research into fiber reinforced concrete had begun

(Banthia & Trottier, 2016). Fibers offer a variety of benefits from blast resistance, to increased tensile strength, and to improved shear resistance. The fibers of today come in many shapes, sizes and materials including synthetic fibers, natural fibers, recycled fibers, and nano fibers.

There has been extensive research done on fiber reinforced concrete. In application, FRC is mostly used where there is some sort of restraint, such as in slabs or in areas where there is confining reinforcement. These applications take advantage of the enhanced matrix toughness with regards to energy absorption, crack control, and durability (Zollo, 1996). The bond of the concrete to fibers is very important to prevent pullout so choosing the right geometry of fiber is critical.

2.3.2 Steel Fibers

Steel fiber reinforced concrete (SFRC) is well known for its superior resistance to cracking and crack propagation. The ductility and added tensile strength make SFRC much tougher as defined by the area under the load vs. deflection curve. While the benefits are great, it must be understood that since the fibers are short and discrete, they cannot be used as a replacement for longitudinal reinforcement. Fibers are meant to improve the cracking, deflection and serviceability of the concrete. The cost of steel fibers, unfortunately, is relatively expensive, costing almost double for a 1% addition. This has limited application to specialty projects such as repair, tunnel linings, and pavement. Another difficulty of fibers is potential for clumping and uneven distributions. Special precautions must be taken to avoid this such as: making sure the fibers aren't clumped while adding, gradual adding of the fibers, avoiding high fiber contents, using a good condition mixer, and adding the fibers at the end (Van Chanh, 2004).

The addition of steel fibers is known to reduce the fluidity and workability of concrete. In SCC, the flowability and passing ability is decreased with the addition of fibers, but can still meet the guidelines of what is considered SCC. There is an upper limit of fiber content where the stiff structure of the granular skeleton makes consolidation under its own weight impossible (Grünewald & Walraven, 2001). The mechanical properties of steel fiber reinforced SCC (SFRSCC) is relatively similar to regular SCC but the difference comes in the mode of failure. In flexural, splitting tensile and compressive tests, SFRSCC demonstrate high ductility and thus prevent sudden failure (Gencel et al. 2011). SFRSCC is also satisfactory from a durability standpoint with a low late of chloride diffusion, thanks to the low porosity, and moderate resistance to freeze thaw (Corinaldesi & Moriconi, 2004).

2.4 Shrinkage Mitigation and Factors in Self Consolidating Concrete

Every component of a concrete mix contributes to the performance of the concrete including: water to cement ratio, use of pozzolans, type of aggregate, admixtures used, fibers, and the environment the concrete is in. It is important to understand how these components each affect the total shrinkage to design a SCC mix with the desired flow and to minimize shrinkage. By minimizing the total shrinkage by even a small degree, there becomes less chance of cracking in restrained conditions and can greatly extend the life of the structure and contribute to lowering the life cycle cost.

2.4.1 Water, Cement and Pozzolans

The water to cement ratio, the amount of cement, and type of cement used are very important to controlling the amount of shrinkage. The hydration reaction between the water and cement is a large component of plastic and autogeneous shrinkage. There has

been plenty of research on the effect of the water to cement ratio on shrinkage, as well as the effect pozzolans have on the hydration reaction that leads to shrinkage.

During autogeneous shrinkage, there is a volume change as a result of the hydration products having less volume than the un-hydrated cement and water. This is sometimes referred to as chemical shrinkage. In cement paste, which is just water and cement, the change in volume is quite large. The aggregate in concrete creates restraint which makes the change in volume much smaller. When the water to cement ratio is high, above .42, the effect of autogeneous shrinkage is very low. When the water to cement ratio lowers, the amount of autogeneous shrinkage steadily increases (Zhang et al. 2003). The higher water to cement ratios provides plenty of water for the hydration process so the change in volume is not as severe.

In SCC, a low water to powder ratio is desired around 0.9 to 1.0 depending on the type of powder (Okamura, 1998). Typical powders used are limestone powder, fly ash, silica fume, and slag. These powders are used to supplement cement to lower the cost and offer a variety of additional benefits depending on what type of powder is chosen. The powders require less superplasticizer than ordinary concrete to reach the desired flow. The powder materials help to maintain sufficient cohesion in the mix and reduce bleeding, segregation and settlement. These powders, or pozzolans, slow down the hydration reaction because they are less reactive than regular cement. This makes having a low water to powder ratio beneficial in decreasing thermal stress and thus lowering shrinkage (Zhu & Gibbs, 2005).

One type of powder commonly used is limestone filler, which is primarily calcium carbonate. Researchers noticed that as the volume of paste increases, the amount of total free shrinkage increases. Researchers were able to achieve a lower free shrinkage while maintaining a high paste volume by replacing some aggregate with the limestone filler. While paste volume has a large effect on shrinkage, it is largely dependent on the paste proportions. Additionally when there is higher water content, the effect on shrinkage versus paste volume is much more prominent as drying shrinkage plays a larger role (Rozière et al. 2007).

Fly ash is a common addition to concrete and is known to increase workability and provide long term strength. Compared to only cement as a binder, a fly ash and cement combination requires less superplasticizer to obtain a desired slump. In a study looking at the effect of strength and shrinkage of different percentages of fly ash as a substitute in SCC, a mix with 40% fly ash had the highest strength and would decrease with higher percentage. Free shrinkage improved significantly as the fly ash content increased with over 50% improvement with fly ash content over 40% (Khatid, 2008). Since fly ash acts as a pozzolan, the hydration process is much long than conventional cement, lowering the heat and limiting autogeneous shrinkage, especially in the early stages. There is a tradeoff at very high percentages of fly ash where increased shrinkage resistance will result in weaker concrete, so it is important to understand the strength needed to see what is the max amount of fly ash that can be substituted. Sometimes it can beneficial to add a combination of pozzolans such as fly ash and silica fume as it has been shown to increase the tensile and compressive strength and modulus compared to just fly ash (Yazici, 2008).

Silica fume is a byproduct of producing silicon metal and has been used as a pozzolan in concrete for years. Unlike fly ash, silica fume demands more superplasticizer, but obtains a higher strength at 28 days than a control mix without silica fume at substitution percentages under 15%. A binary cementitious blend of silica fume and cement does not improve drying shrinkage as much as other blends. To make a mix with greater shrinkage control using silica fume, it must be used in conjunction with other types of pozzolans (Gesoğlu et al. 2009). Metakaolin is another supplementary cementing material that acts like silica fume. Since metakaolin can be produced, a higher purity can be achieved to react better with the calcium hydroxide formed during Portland cement hydration. Because of this, metakaolin can achieve higher strength and less shrinkage at up to 15% replacement (Hassan et al. 2012).

Ground granulated blast furnace slag, is a byproduct from the steel industry and is used as a replacement for cement in concrete. Slag is a very fine powder that delays hydration and fills up pores. This makes slag effective at lowering both autogeneous shrinkage early on and can help lower drying shrinkage over time. When slag is used a replacement in varying amounts, the strength is very similar. The compressive strength increases when either silica fume or metakaolin are used in addition to slag as a substitute to cement. In terms of shrinkage, slag as binary blend performs better than silica fume and ordinary cement, but poorer than fly ash or metakaolin regardless of water to cement ratio. In a general linear model analysis of variance looking at many different cement combinations, silica fume had the highest contribution to drying shrinkage followed by metakaolin, fly ash, and slag (Güneyisia et al. 2010).

2.4.2 Aggregate

An SCC mix calls for a higher fine to coarse aggregate ratio than ordinary concrete, and smaller maximum aggregate size to help achieve the high workability. A lower coarse aggregate count results in higher shrinkage. Concrete shrinkage can be predicted with a Pickett model using Equation 2.1 (Wei et al. 2011):

$$\varepsilon_C = \varepsilon_P * (1 - V_A)^n \qquad (2.1)$$

Where, ε_C is shrinkage of concrete

ε_P is shrinkage of the paste

V_A is the volume fraction of the aggregates

n is a correlation parameter controlled by aggregate restraining effects

From this equation it is clear that regardless of the shrinkage properties of the concrete paste, a higher fraction of coarse aggregate will cause a higher concrete shrinkage. To obtain a low shrinkage SCC mix, a high amount of aggregate must be used but not too much to compromise with the flowability.

Lightweight aggregates, such as pumice have been shown to greatly decrease autogeneous shrinkage. Lightweight aggregates are typically porous and can be presoaked with water. Water that is lost by self desiccation can be replaced with the water from the lightweight, soaked aggregate. This internal curing is most effective when there are small spaces between the aggregates. This allows the cement paste to easily access the water from the aggregate. The right size aggregate and absorption can effectively eliminate self desiccation entirely (Zhutovsky et al. 2002).

2.4.3 Admixtures

Admixtures are added to concrete to change the concretes properties. They come in both liquid and solid forms and vary based on the property they are trying to adjust. Years of advancements have allowed the formulation of admixtures that can tackle various concrete properties. This includes, but not limited to, the workability, setting time, permeability, air entrainment, and color.

Superplasticizers, such as high-range water reducers are vital in SCC to improve workability without increasing the water to cement ratio. This keeps the water content low but leaves the concrete susceptible to autogeneous shrinkage. Different water reducers types can are better at controlling shrinkage than others. Polycarboxylate-based water reducer shows a better effectiveness than other types at reducing plastic shrinkage and early evaporation. This happens because the water reducer lowers the rise of capillary pressure at early age. The lower capillary pressure is also beneficial for preventing early age cracking (Qin et al. 2012).

To directly reduce shrinkage, shrinkage reducing admixtures (SRA) have been developed. SRAs work by decreasing water surface tension, and they delay and extend the hydration process. As a result, setting time is delayed and temperature is decreased, which greatly reduces both autogeneous and plastic shrinkage. The effectiveness varies for each particular mix, but in general, a higher SRA content will result in less shrinkage and higher durability. The increased SRA content has the negative effect of lower strength, especially at early ages (Maia et al 2012). In addition to lower strength, the current cost of SRA is quite expensive and must be considered when creating an

economic SCC mix. A cost benefit analysis shows that the addition of SRA can increase the total cost of the concrete by 16% (Rodden & Lange, 2004).

2.4.4 Fibers

Fibers are included in concrete to increase toughness and provide ductility. Fibers, such as polypropylene (PP), have been shown to be effective at preventing plastic shrinkage. The advantages are larger when curing is limited. The addition of PP showed no difference in the shrinkage of concrete cured for seven days, while one day curing showed clear benefits in overall shrinkage. PP makes the concrete more permeable and increases the nano porosity raising the rate of drying and drying shrinkage. This is slightly offset by the slight increase in tensile strength (Aly et al. 2008). In SCC, the use of fibers to lower shrinkage and shrinkage reduced cracking has been promising. PP fibers and steel fibers have proved to be effective in counteracting early age cracking and drying shrinkage, with PP being most effective at early age and steel at the delayed drying shrinkage (Corinaldesi & Moriconi, 2011). The high cement and low aggregate amount of SCC will certainly cause high shrinkage, so effective use of fibers can help to achieve a low shrinkage fiber reinforced self consolidating concrete mix.

2.4.5 Environmental Factors

Many of the different modes of shrinkage are dependent on the evaporation of water in concrete. It is no surprise that the temperature and environment play a large role in minimizing shrinkage. Generally, high temperature and low humidity will accelerate evaporation and lead to very high levels of early age autogeneous shrinkage. To minimize autogeneous shrinkage, the concrete must constantly be in the presence of water. One way of achieving this is to moist cure the concrete. In the early stages as the

concrete undergoes hydration, the outside water source can be utilized and shrinkage can be delayed. Wet curing should be done as soon as hydration begins and end when depercolation of the capillaries occur. Although construction conditions and costs may prevent long, extended curing, just a couple days of wet curing can result in substantial improvements in the mechanical properties of the hardened concrete (Bentz & Jensen, 2004).

2.5 Restrained Shrinkage Ring Test

There are a couple ways to evaluate concrete's shrinkage performance under restrained conditions. One of the most popular is the steel ring test. The test involves a steel ring with concrete casted around it creating restrained conditions. There are two types of rings, one developed by AASHTO and other by ASTM. The test is primarily used for comparative studies to compare difference in cracking behavior between different mixes. The low cost and simple set up make it a valuable research tool for research and quality control, but does not give quantitative information on stress development or the prediction of cracking in real-life situations.

2.5.1 AASHTO Ring

In 1998 AASHTO accepted the ring test as a provisional standard as "AASHTO PP34-98: Standard Practice for Estimating the Cracking Tendency of Concrete". The test uses time of cracking to determine the restrained shrinkage performance of a variation of parameters in concrete. These parameters could be aggregate type, cement type, water content, admixtures, or fibers. The procedure consists of casting a 3" thick concrete around the circumference of a steel ring with a height of 6", inner steel diameter of ½" +/- $^{1}/_{64}$", and outer steel diameter of 12". The surfaces of the steel must be polished and

smooth to ensure a consistent bond of the concrete and ring. On the inside diameter of the ring, four foil strain gauges (FSG) are installed at mid height to measure the strain in the steel. The gauges connect to a data collection system and the rings are left in temperature and humidity controlled room. The rings are monitored every few days for indications of cracking. When a crack occurs, the day to cracking is noted and the crack width and propagation are monitored. Cracks may not always occur within 28 days especially in low shrinkage mixes, so modifications to the test can be made. For the AASHTO ring, a max aggregate size of 1" must be used, which makes the test applicable to most concrete mixes.

Knowing the dimension of the ring and strain in the steel at a given time, the strain in the concrete can be inferred. A study by Hossain & Weiss (Hossain & Weiss, 2004) developed the following relationship below in Equation 2.2.

$$\sigma_{actual} = -(t) * E_s * C_{3r} * C_{4r} \qquad (2.2)$$

Where, (t) *is the strain in the steel at time* t

E_s *is the elastic modulus of steel*

$C_{3r} = (R_{OS}^2 + R_{OC}^2)/(R_{OC}^2 - R_{OS}^2)$

$C_{4r} = (R_{OS}^2 - R_{IS}^2)/2R_{OS}^2$

R_{OS} *is the outer radius of the steel ring*

R_{IS} *is the inner radius of the steel ring*

R_{OC} *is the outer radius of the concrete ring*

2.5.2 ASTM Ring

Similar to AASHTO, the American Society of Testing Materials (ASTM) developed a similar test method. The main difference comes in the geometry of the steel ring. The steel ring used has a wall thickness of ½" ± 0.05 in, an outside diameter of 13.0" ± $^{1}/_{8}$" in, and a height of 6.0" ± 0.25 in. The concrete thickness will be smaller at 1.5". There must be a minimum of 2 strain gauges to record the strain development. The smaller thickness of concrete and larger concrete radius provides a larger restraint and accelerates the time to cracking compared to the AASHTO ring test. The drawback of the ASTM test is that it limits the maximum coarse aggregate size to .5". The testing procedure is almost identical to the AASHTO test so it is possible to monitor both ring specimens simultaneously with the same data collection system as long as the aggregate requirement is met.

2.6 Summary of Previous Work

The restrained shrinkage test is a good comparative test to observe the cracking resistance of concrete under restrained conditions. Researchers typically choose a variable to adjust and cast multiple rings to observe when cracks form under similar conditions. In addition to the timing of cracks, the crack width, propagation and distribution can help determine the effectiveness of a mix to resist shrinkage induced cracking. Directly observing the shrinkage behavior is not enough to understand the development and propagation of cracks so utilizing the ring test is important to greatly understand the cracking potential of a mix. In a study looking at the influence of paste volume on restrained shrinkage, researchers noticed that there is not always a correlation between free shrinkage results

and stress development in the ring tests. The stress development is dependent on both shrinkage and the visco-elastic properties of the concrete (Roziere et al. 2007).

SCC typically shrinks more than conventional concrete due to the higher cement paste. At identical water to cement ratio, SCC has a lower elastic modulus and higher susceptibility to early age shrinkage cracking under restrained conditions compared to conventional concrete (Leemann et al. 2011). SCC shows a higher stress development especially in the early age of the restrained shrinkage test and all cracked before 28 days, unlike the conventional concrete which showed and slower stress development with no clear cracks. The study also saw large variance in shrinkage performance based on the cement type use. The cements using pozzolans greatly increased the cracking resistance over the ordinary Portland cement mix. The ring test shows that early age cracking is a large issue with SCC and efforts to reduce shrinkage cracking must be taken to be an effective alternative to HPC.

In attempts to improve the restrained shrinkage performance of SCC, fibers and/or SRA can be added. A study by Hwang and Khayat used the ASTM ring test to investigate the influence of HRWR, PPE fibers, SRA, and hybrid fibers on shrinkage cracking. Their results showed that an increase of PPE fiber content of .25% by volume would lead to an approximately 40% decrease in time to cracking. They also found that the addition of SRA lowered drying shrinkage by 40% at 56 days and decreased time to cracking 2.4 folds compared to SCC without SRA. A combination of SRA and fibers were found to be most effective in delaying cracking (Hwang & Khayat, 2008).

When fibers are added, the level of complexity in the concrete rises. In a study by Shah and Weiss, acoustic emission testing was used in the ring test to observe microcracking in concrete with varying fiber amounts. The researchers found that fibers have little influence on stress development before cracking. The fibers are able to delay visible cracking because of their ability to resist the microcracks from propagating outwards. Because of this, fibers can permit higher stresses before cracking is visibly observed. In the time before the crack becomes visible, the strain does decrease a little. In high fiber contents, it is difficult to determine the days to cracking because the fibers prevent the microcracks that form to propagate. In concrete without fibers, the strain and stress plateau before cracking as multiple microcracks form until a large visible crack forms resulting in a large loss in strain. The researchers also noticed that as fiber volume is increased, crack width decreases until a point where it begins to level off (Shah & Weiss, 2006).

Not many studies have utilized both the AASHTO standard ring and ASTM ring, but there have been studies that look at the influence of ring geometry on stress development. Both standards call for circumferential drying although some researchers have modified the test to allow top to bottom drying. Hassain and Weiss looked at stress development on various ring and specimen geometries including both steel thickness and concrete thickness. They found that a thin steel thickness (1/8”) did not provide enough restraint and provided lower stress than thicker steel rings. The researchers also found that varying concrete thicknesses had little effect on stress development but clear differences in days to cracking. The 3” thick concrete (as per AASHTO) took about twice as long to crack compared to the 1.5” thickness concrete (as per ASTM). This trend continued for larger

concrete thicknesses and is similar for both circumferential and top to bottom drying (Hossain & Weiss, 2006).

In an effort to directly measure the strain in the concrete during the restrained shrinkage ring test, strain gauges can be directly embedded into the concrete. By directly embedding strain gauges in the concrete, the stress distribution can be visualized. It is not unusual for concrete to exhibit uneven stress distribution and this method can be used to predict when and where a crack will form. In a study by Ghanchi and Nassif, 6 vibrating wire strain gauges (VWSG) in the shape of a hexagon were embedded directly into the concrete of an AASHTO ring. They studied the effect of polypropylene fibers in SCC. The use of VWSG was a used successively as a supplement to the FSG data. The VWSG accurately predicted the region in which the crack will form before it could be visually seen. The embedded VWSG did not affect the days to cracking but may influence cracking to occur near the embedment areas (Ghanchi & Nassif, 2015). When analyzing FRSCC, cracks do not always become visible right away so the strain gauges are important in picking up these microcracks that eventually lead to full propagated cracks. The FSGs can show a slight decrease in strain before the crack shows and the VWSG can indicate high tension as an indicator of potential cracking before the crack can be visualized. The combination of strain gauges helps give a better understanding of the concretes behavior under restrained shrinkage.

CHAPTER III

3 EXPERIMENTAL PROGRAM

3.1 Introduction

The experimental program for this study consists of mixing concrete, testing for fresh properties, casting samples, testing for mechanical properties and testing for shrinkage properties. The fresh properties to be looked at are slump, T20, VSI, and J-ring performance. The mechanical properties to be tested include compressive strength, tensile splitting strength, and modulus of elasticity. The shrinkage performance will be assessed by free shrinkage testing and the restrained shrinkage ring tests. There will be four SCC mixes in which two parameters will vary; the amount of HRWR and fiber content. The HRWR is added to reach the desired workability requirements. The tests were performed according to ASTM and/or AASHTO specifications.

3.2 Material Properties

Materials used in the mix obtained from various local providers. All materials were chosen with easy accessibility in mind since the final product is intended to be used by local transportation agencies. The coarse aggregate and cement, used in the mixes are obtained from Clayton Concrete in Edison, NJ. Grade 120 slag was obtained from LaFargeHolcim in Bayonne, NJ. Admixtures, including air entrainer and superplasticizer, and fibers were provided by Euclid Chemical in East Brunswick, NJ. A summary of materials and suppliers are provided below in Table 3.1:

Table 3.1 Materials and Suppliers

Material	Type	Supplier
Fine Aggregate	Concrete Sand	Clayton Concrete
Coarse Aggregate	#8 (3/8”) Granite	Clayton Concrete
Cement	Portland Type I	Clayton Concrete
GGBFS	Grade 120	LaFargeHolcim
Air Entrainer	AEA-92S	Euclid Chemical
Superplasticizer	Plastol 5000	Euclid Chemical
Fibers	PSI Crimped Steel 1.5”	Euclid Chemical

The fine and coarse aggregates were tested for specific gravity, fineness modulus, and absorption as per ASTM C 127 and ASTM C 128. The moisture content is also taken before each mix. The results of these results are shown below in Table 3.2.

Table 3.2 Aggregate Properties

Properties	Fine Aggregate	Coarse Aggregate
Specific Gravity	2.62	2.83
Fineness Modulus	2.35	6.03
Absorption	1.10%	0.40%
Moisture Content (varies)	.61-2.59%	0.23-1.38%

The cement used is Portland type I and conforms to ASTM C 150. This standard guarantees that the cement will meet chemical composition, physical properties, reactivity and strength requirements. Similarly, the distributer of the slag guarantees that grade 120 slag conforms to ASTM C 989 requirements. The superplasticizer used is a polycarboxylate based high-range water reducer. The brand name used from Euclid is Plastol 5000 and complies with ASTM C 494 and AASHTO M 194 Type F admixture and ASTM C 1017 as a Type I admixture. The air entrainer used Eucon AEA-92S from Euclid Chemical and meets or exceeds the requirements of ASTM C 260 and AASHTO M 154. The fibers used are a steel macro fiber shown in Figure 3.1. In particular, the fiber

used is PSI Crimped steel fiber from Euclid Chemical. The fiber complies with ASTM C 1116 and ASTM A 820 and the technical information provided by the manufacturer is listed below in Table 3.3.

Figure 3.1 Crimped Steel Fiber

Table 3.3 Steel fiber properties

Material	Low carbon cold drawn steel wire
Aspect Ratio	34
Length	1 1/2 in.
Tensile Strength	140-180 ksi
Relative density	7.7

3.3 Mix Proportions

There will be a total of 5 mixes to be compared for this study. One control SCC mix without fibers and four FRSCC mixes with increasing amounts of fiber. These mixes are

each done twice, with the exception of set B which does not include the fourth FRSCC mix, and are split into set A and set B. Set A will be cured for 7 days and set B will be cured with a one day wet cure. The mix proportions of the control mix are based on the studies and findings of the Virginia Transportation Research Council (Brown et al. 2008). This is the same mix proportions in the study by Ghanchi and Nassif, but difference will come in the use of steel fiber instead of polypropylene. A summary of the mix proportions for each mix is shown below in Table 3.4.

Table 3.4 Summary of Mix Proportions

Mix	ST 0.00	ST 0.35	ST 0.50	ST 0.65	ST 0.80
CM lb/cy	439	439	439	439	439
Slag lb/cy	236	236	236	236	236
Rock lb/cy	1436	1436	1436	1436	1436
Sand lb/cy	1436	1436	1436	1436	1436
Water lb/cy	288	288	288	288	288
AEA oz/cwt	2.0	2.0	2.0	2.0	2.0
HRWR oz/cwt	12.0	12.0	13.0	13.0	14.1
Fiber %by volume	0.00	0.35	0.50	0.65	0.80
W/C	.425	.425	.425	.425	.427

The mix proportions were kept identical for all mixes. The only variable that changes is the fiber content and HRWR content. The total cementitious material used is 675 lb/cy with a water to cement ratio of .425. Grade 120 slag accounts for 35% of the total cement while the rest is Portland type I cement. The amount of coarse aggregate and fine aggregate are kept the same at 1436 lb/cy, hence the coarse to fine aggregate ratio is 1:1. There are four fiber volumes being investigated. ST 0.00 refers to the control mix with no fiber, and ST 0.35, ST 0.50, ST 0.65 and ST 0.80 contain 0.35, 0.50, 0.65 and 0.80 percent fiber by volume. Since the added fibers decreases workability, ST 0.50 and ST

0.65 needed a higher amount of HRWR increasing from 12 oz/cwt to 13 oz/cwt and ST 0.80 increased up to 14.1 oz/cwt.

3.4 Mixing and Test Methods

3.4.1 Introduction

Each mix will be batched and mixed in a 6cf capacity mechanical drum mixer. A representative sample will be taken from the mix and fresh properties will be tested. To ensure that the mix meets the workability requirements of SCC, a number of tests will be performed including the slump test, T20, VSI, and J-ring. If the mix does not have the desired flowability, additional HRWR will be added to achieve the desired flow. If there are problems with segregation or bleeding, a note will be taken of the severity. After the tests are performed, a various number and type of samples will be taken. After curing, mechanical properties will be tested, and shrinkage will be closely monitored.

3.4.2 Mixing Procedure and Fresh Properties

A day before a scheduled mix, the materials are batched and stored in buckets. The moisture content of the coarse and fine aggregate are taken to ensure the proper water content of the mix. The batching will then be adjusted after the moisture content is calculated. The total quantity of concrete per mix is approximately 3 cubic feet. For all mixes the same mixer is used as shown in Figure 3.2.

Figure 3.2 Mechanical Drum Mixer Used

Before the mix starts, the mixer is buttered by wetting the mixer. This helps to prevent the concrete from sticking to the sides and ensuring a well-mixed concrete. Before adding anything to the mixer, the AEA is mixed into the bucket of batched water. All the aggregate is then added to the mixer and mixed for 1 minute or until properly mixed. 1/3rd of the water is then added and mixed for 2 minutes ensuring that no aggregate gets stuck on the sides. The cement and slag are then added together. After the cementitious materials are in the mixer, the rest of the water is slowly added as the mixer is turned on. After the water is added, the components are mixed for 3 minutes. At each minute interval, the sides of the mixer are checked for any stuck materials and are scraped off. After the 3 minutes are up, the concrete rests for 2 minutes. Then all the HRWR is added

to the mixer and mixed for 2 minutes followed by a resting period of 3 minutes. After the 3 minutes rest, fibers are slowly added (if applicable) as the mixer is turning, making sure there are no clumping of the fibers. Mixing occurs for another 2 minute or until there is an even distribution of fibers. The concrete is then ready for testing for fresh properties.

3.4.2.1 Slump Test (ASTM C 1611)

The slump test will be performed following ASTM C 1611. The slump test performed is similar to the slump test described in ASTM C 134 which is applicable to conventional concrete. The same slump cone, strike off rods and base plate are used but the procedure is different. Because SCC can consolidate under its own weight, there is no rodding of the concrete. The cone is also inverted so that the smaller end is on the ground as seen in Figure 3.3. When the cone is raised, the concrete flows radially forming a flat disk shape. Unlike ASTM C134, ASTM C 1611 measures the slump horizontally instead of vertically. The slump is measured by measuring averaging the largest diameter and the diameter that is 90 degrees offset from the largest diameter as seen in Figure 3.4. Typically a slump over 20” is desired for SCC.

Figure 3.3 Inverted Slump Cone

Figure 3.4 Measuring Slump (ASTM C1611)

3.4.2.2 T20 Test

To further assess the workability of an SCC mix in addition to measuring the max diameter from the slump test is to understand how quickly the concrete can flow. Researchers typically use the T20 time to gauge the flowability of an SCC mix. The T20 time is defined as the time in seconds it takes the concrete to reach a 20" diameter circle on the base plate after lifting the slump cone. The time is recorded to the nearest tenth of a second.

3.4.2.3 Visual Stability Index (VSI)

An important quality of SCC is that it can resist segregation and bleeding despite its high paste and workability. To gauge the concretes resistance to segregation and bleeding, a Visual Stability Index (VSI) is used that is based on visual observation and inspection. After the slump test and before clearing the base plate, the concrete is checked for signs of segregation or bleeding and is given an index number of 0 to 3. An index of 0 means there is no evidence for segregation or bleeding. An index of 1 means there is slight bleeding in the form of sheen on the concrete. An index of 2 means there is a slight mortar halo around the edges under a half inch. An index of 3 means there is a mortar halo in excess of a half inch around the edges. A VSI of 2or 3 is considered unstable.

3.4.2.4 J-Ring Test (ASTM C 1621)

The J-Ring test is a test method that determines the passing ability of SCC. The test is done in accordance to ASTM C 1621. After the slump flow, T20, and VSI are noted, the slump is then taken again with some minor adjustments. To imitate the presence of rebars and tight spacing, a 12 inch diameter metal ring with 16 vertical bars are placed on the base plate around the slump cone as shown In Figure 3.5. The slump cone is then filled

and lifted the same way according to ASTM C 1611. The concrete then is allowed to flow until it stops, there is no need to record the timing. With the J-Ring still in place, the largest diameter is recorded followed by the 90 degree offset diameter as seen in Figure 3.5. These values are then averaged together and are reported as the J-Ring flow. This value will be compared to the slump flow calculated during ASTM C 1611. A difference in flow of less than 1 inch indicates no visible blocking. A difference in flow in-between 1 and 2 inches indicates minimal to noticeable blocking. A difference in flow greater than 2 inches indicates extreme blocking.

Figure 3.5 (a) J-Ring test (b) J-Ring flow

3.4.2.5 Sampling (ASTM C 172) and curing

The size of the mix is determined such that there is enough concrete to fill all the required samples. There are two sets of mixes per fiber content. The first set contains all cylinders and will be subject to a 7 day wet cure. The second set will include a number of different types of samples. These samples include at least 12- 4”x8” cylinder molds for strength

testing, 3- 3”x3”x10” free shrinkage prisms, 2- AASHTO rings with an inner concrete diameter of 12”, an outer concrete diameter of 18 inches and 6 inch height, and 1 ASTM ring with an inner concrete diameter of 13”, an outer diameter of 16 inches and a height of 6 inches. The restrained shrinkage molds are assembled beforehand and are shown in the Figure 3.6. Careful attention must be taken to ensure the ring and outside mold are centered such that an even thickness of concrete is casted. The samples are casted after J-Ring test concludes. The molds are filled to the top and there is no need for any vibration or compacting.

Figure 3.6 (a) AASHTO Ring setup (b) ASTM ring setup

After casting, the molds are covered and stored in an environmental chamber kept at a constant 75 degrees Fahrenheit and 50% humidity as shown in Figure 3.7. For the rings which have no cover on top, wet burlap is added in addition to plastic sheets to ensure a wet cure. After demolding, the free shrinkage molds and cylinders are moved to a curing room and placed in a water tank shown in Figure 3.8 to cure for one extra day to reduce autogeneous shrinkage and gain more strength. The rings are demolded and sealed so that

the only concrete exposed to the air is on the circumference. So, to simulate wet curing, wet burlap covered the outside of the ring for one more day. After the one additional day of wet curing, all strength and shrinkage samples are put in the environmental chamber for the remainder of the test.

Figure 3.7 Environmental Chamber

Figure 3.8 Water Curing Bath

3.5 Laboratory Testing

A number of mechanical properties are tested for in addition to the fresh properties. The tests include compression tests, tensile splitting tests, modulus tests, free shrinkage testing, and restrained shrinkage testing. The first set of mixes was tested for compression, tension, and modulus with 7 day wet curing. The second set of mixes was tested for compression, tension, free shrinkage, and restrained shrinkage with one day wet curing. A summary of the tests performed in this study, including fresh properties, mechanical properties, and shrinkage properties, along with the applicable testing standards are provided in Table 3.5. The table provides a summary for the tests performed for each fiber amount, with the exception of ST0.80 which did not undergo the second set of testing due to lack of workability.

Table 3.5 Laboratory Test Summary for Each Mix

Test	Applicable Standard	Number of Specimens		Age of Concrete, Days	
		Set A	Set B	Set A	Set B
Slump, T20, VSI	ASTM C 1611	1	1	0	0
J-Ring	ASTM C 1621	1	1	0	0
Compressive Strength	ASTM C 39	10	8	1,7,14,28,56	2,7,14,28
Tensile Splitting	ASTM C 496	10	8	1,7,14,28,56	2,7,14,28
Modulus of Elasticity	ASTM C 469	4	0	7,28	n/a
Free Shrinkage	ASTM C 157	0	3	n/a	1 through 91
Restrained Shrinkage	AASHTO T334	0	2	n/a	1 through 28
Restrained Shrinkage	ASTM C 1581	0	1	n/a	1 through 28

3.5.1 Compression Strength Test (ASTM C 39)

Compressive tests were done at 1 day, 7 day, and 28 days, and sometimes 14, 56, and 91 if there are extra cylinders for set A with the 7 day wet curing. For set B, tests were performed at minimum 7 and 28 days. The standard used is ASTM C 39. To ensure a level and consistent surface, the 4”x8” concrete cylinders are capped with a sulfur based capping compound as seen in Figure 3.9. The standard followed for capping is ASTM C 617. The capped cylinder is then put in a compression machine shown in Figure 3.10 and loaded until failure. A minimum of 2 cylinders are used to ensure consistency and accuracy.

Figure 3.9 Sulfur Capping

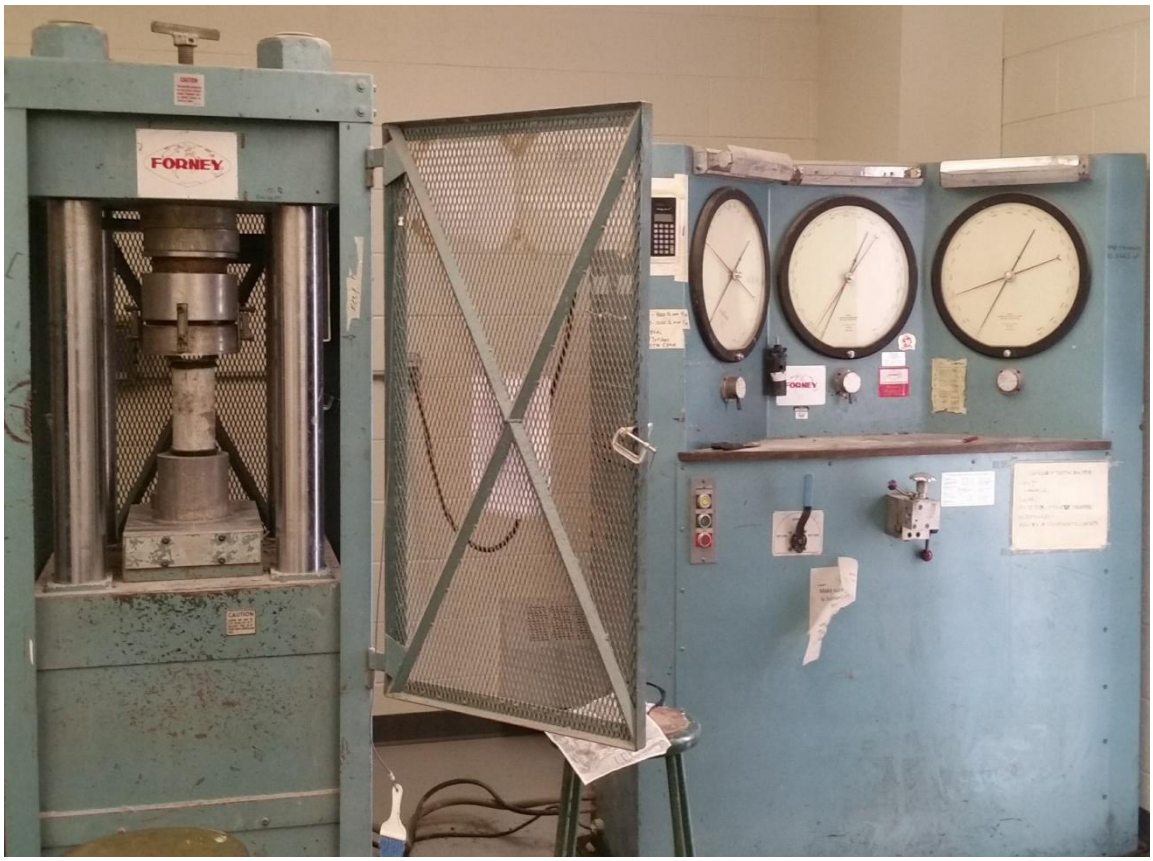

Figure 3.10 Compression Machine for Compression, Tension, and Modulus Testing

3.5.2 Tensile Splitting Testing (ASTM C 496)

Tensile testing is done according to a similar schedule with compression testing. A 4”x8” cylinder is placed horizontally in the testing machine and is loaded according to ASTM C 496. The specimen is then tested until failure. For specimens without fiber, failure is clear as the specimen will crack down the middle and no additional load can be taken by the cracked concrete. When fibers are added, the specimen will crack but will remain intact due to its ductility and ability to resist full splitting. After FRSCC cracks, the specimen will continue to take load as the contact surface area increases as seen in Figure 3.11. It is important to note that that higher load is not the load to calculate the tensile splitting strength. For this study, the load at which the concrete initially cracks is the one that will

be used to determine the tensile splitting strength. A minimum of 2 specimens will be tested to ensure accuracy.

Figure 3.11 Splitting of FRSCC Specimen

3.5.3 Modulus of Elasticity Testing (ASTM C 469)

The modulus testing was done for the first set of mixes at 7 and 28 days. The test was performed according to ASTM C 469. Similar to the compression samples, the specimens are sulfur capped according to ASTM C 617. To begin the test, the compression tests must be concluded. The modulus sample is connected to a cage by a number of small screws as seen in Figure 3.12 and is loaded to 40% of its compressive strength and then unloaded. The cage distance on opposite sides is then measured with a caliber. The sample is then loaded and the deflection of the cage is taken at even load increments by a length comparator. This is done twice for each cylinder tested.

Figure 3.12 Elastic Modulus Cage

3.5.4 Free Shrinkage Testing (ASTM C 157)

For each mix in set B, at least 2 free shrinkage molds were made. The steel molds have metal studs screwed in that embed themselves into the concrete when casted and then demolded. After the 3”x3”x10” prisms are demolded and a half hour at least has passed, the first measurements are taken. Using a length comparator and a reference bar as shown in Figure 3.13, the initial gauge reading is taken three times for each sample. After these measurements, the samples are put into a water bath to cure for one day. The next day after 24 hours, they are taken out and let to dry before the next measurements are taken.

Subsequent measurements are taken periodically with more frequency in the early ages as the concrete is most prone to free shrinkage during that time. Free shrinkage was measured up to 91 days.

Figure 3.13 Free Shrinkage Testing

3.5.5 Restrained Shrinkage Testing

In addition to the strength specimens and free shrinkage specimens, a total of 3 restrained shrinkage rings will be casted. There will be 1 ASTM ring and 2 AASHTO rings. The 2 AASHTO rings will be modified with 6 additional VWSGs to supplement the standard setup. The rings are prepped with the proper molds and strain gauges, casted, sent to the

environmental chamber, demolded, connected to a data collection system, cured with burlap for one additional day, and monitored for signs of cracking up until 28 days.

3.5.5.1 ASTM Restrained Shrinkage Testing (ASTM C 1581)

ASTM C 1581 is a standard test method to determine the age at cracking and induced tensile stress characteristics of concrete and mortar under restrained shrinkage. Each mix in set B will have one designated ASTM ring tested. The maximum aggregate sized applicable is ½" which is larger than the 3/8" used in this studies mixes. To create the setup for the ring rest a number molds and materials must be used. The steel ring used has a thickness of ½", an outer diameter of 13", and is washed and cleared of any concrete or dirt on the outside. Attached will be 4- 120 Ohm foil strain gauges (FSG) equally spaced at mid height on the inner diameter of the steel ring. Foil strain gauges vary in shape and orientation but all work under the same principle. When the guage under goes stress and strain, the whore circuit enlarges or shortens. This change in length causes a change in resistance and hence the current. The strain then can be calculated, with a given guage factor, based on the change in resistance. The FSGs are applied according the manufacturers recommended procedure and products as shown in Figure 3.14.

Figure 3.14 Materials Used for Installing FSGs

The base of the mold consists of a wooden ply board with four pieces of wood attached to create a 16”x16” square. The square should be big enough such that 16” diameter sonotube tubing can snugly fit. The sonotube will be the outside mold for the concrete. The steel ring will then be placed in the center using pre-placed screws to guide the ring to the center position. The final setup for the ASTM ring is shown in Figure 3.15.

Figure 3.15 Final Setup for ASTM Ring

The concrete is then poured into the ring without any compaction or vibrating to the top. The ring is then covered with burlap and a plastic sheet and transferred to the environmental chamber. The rings are then taken off the wooden mold and placed on a plexiglass surface. The top surface of the concrete is then coated with paraffin wax to prevent drying from the top of the ring. The sonotube is then taken off and bottom of the concrete is sealed to the plexiglass surface using a caulk. During this time, the strain gauges are connected to the data collection system. The final setup is shown in Figure 3.16.

Figure 3.16 Final Casting and Placement of ASTM Ring

After everything is demolded and sealed, wet burlap is wrapped around the ring to simulate a wet cure for 1 day. The ring is then observed daily for signs of cracking. When a crack is formed, the crack width and propagation is monitored until the end of the test. At 28 days the full ring is crack mapped and final crack widths are noted.

3.5.5.2 Modified AASHTO Restrained Shrinkage Testing (AASHTO T334)

This study will use 2 AASHTO rings per mix for set B. The AASHTO ring test is similar to the ASTM ring test but is known for taking a longer time to achieve cracking. This is due to the smaller ring diameter (12”) and larger concrete thickness (3”). The benefit of the AASHTO ring is that it is applicable to aggregate sizes up to 1”. The set up is similar to the set up of the ASTM ring. On the inside diameter of the ring, four foil strain gauges are applied at mid height equally spaced out. They are protected by an epoxy and connected to wires which will be connected to a data collection system when the test begins. In addition to FSGs, this study will also include a set of 6 vibrating wire strain gauges (VWSG) embedded to directly measure the strain in the concrete.

The VWSG are placed in the shape of a hexagon and get embedded via bolts. The VWSG used in this study are manufactured by Geokon Inc shown in Figure 3.17. A long metal string is encased by a hollow tube and anchored at the ends. A plucking coil attaches to the sensor and causes the string to vibrate. Small changes is the length change the tension in the wire and hence the frequency of the wire changes. The coil then reads the frequency and is converted to strain given a gauge factor provided by the manufacturer. To prep the ring and sensors for the mix, the hexagon is assembled by forming a hexagon shape with VWSGs. As the concrete shrinks or expands, it will move the bolts, slightly changing the distance in the wire and the plucking coil can measure the strain when connected to a data collection system.

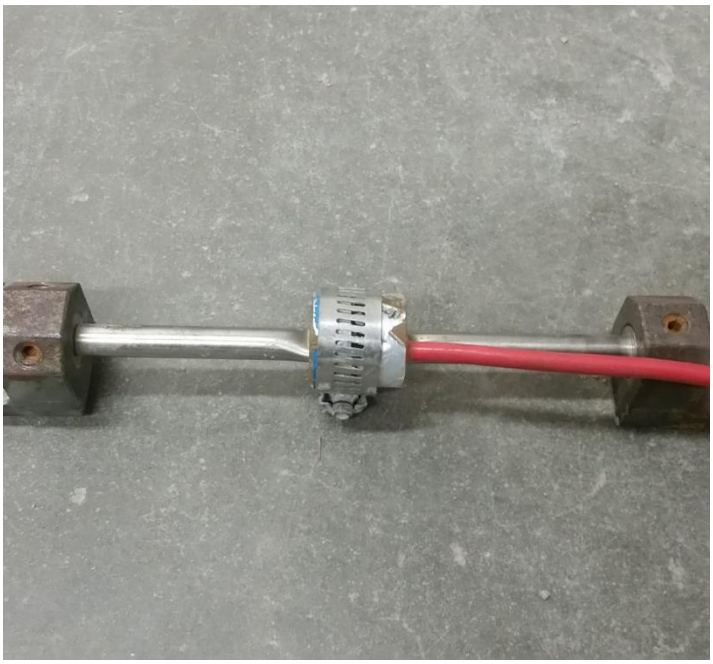

Figure 3.17 Geokon VWSG with Attached Plucking Coil

The wooden molds used are similar to the molds used for the ASTM ring. The difference is in the dimensions. The square must be 18”x18” to fit the 18” sonotube. The

sonotube for both ASTM and AASHTO rings were provided by Clayton Concrete. The pre-placed screws are adjusted such that the 12” outer diameter steel ring is centered.

The concrete is then poured into the mold with no compaction or vibration to the top and smoothed with a dowel. The hexagon is then carefully lowered into the concrete using a metal bars as a guide to ensure the concrete does not touch the sensor and only the bolts touch the concrete. After the VWSGs are lowered, burlap and a plastic sheet cover both AASHTO rings and are transferred to the environmental chamber. After 24 hours in the chamber, the rings are taken off the wooden mold and transferred to a plexiglass shelf. Parrafin wax is melted and applied on the top surface, making sure no wax gets on the sensors. The sonotube is then ripped off and caulk is used to seal the concrete to the plexiglass. The plucking coils which are connected to the data collection system is attached and clamped to the VWSGs. The FSGs are then connected to the data collection system. The rings are then covered in burlap for one addition day to cure. The final setup is shown in Figure 3.18.

Figure 3.18 Final Casting and Placement of AASHTO Ring

The test continues for 28 days and is monitored for signs of cracking. The use of VWSGs, FSGs, and visual inspection help to differentiate between outside noise and actual cracking. When a crack forms, the crack width and propagation is closely monitored for the remainder of the test. At 28 days the ring is fully mapped for any small cracks that the data could not pick up.

3.5.5.3 Sensors and Data Collection System

In total there will be four mixes in set B. Each mix will have 1 ASTM Ring and 2 AASHTO rings. Each mix will require the connection of 12 FSGs and 12 VWSGs. The standards for each test require a maximum of 30 minutes between each strain reading. To collect all this data, a data logging system was created with the capacity to take up to 32 FSG and 64 VWSGs at a time in 4 minute intervals. The modular system shown in Figure

3.19 is comprised of a number of Campbell Scientific products. For the FSGs, the wires are connected to AM16/32 boards which connect to the CR1000 database. For the VWSGs, the wires are connected to AM16/32 boards which connect to an AVW to convert the frequency to strain and then are connected to the CR1000. The whole program was setup using PC200W software where data can be downloaded and sent to Excel for interpretation.

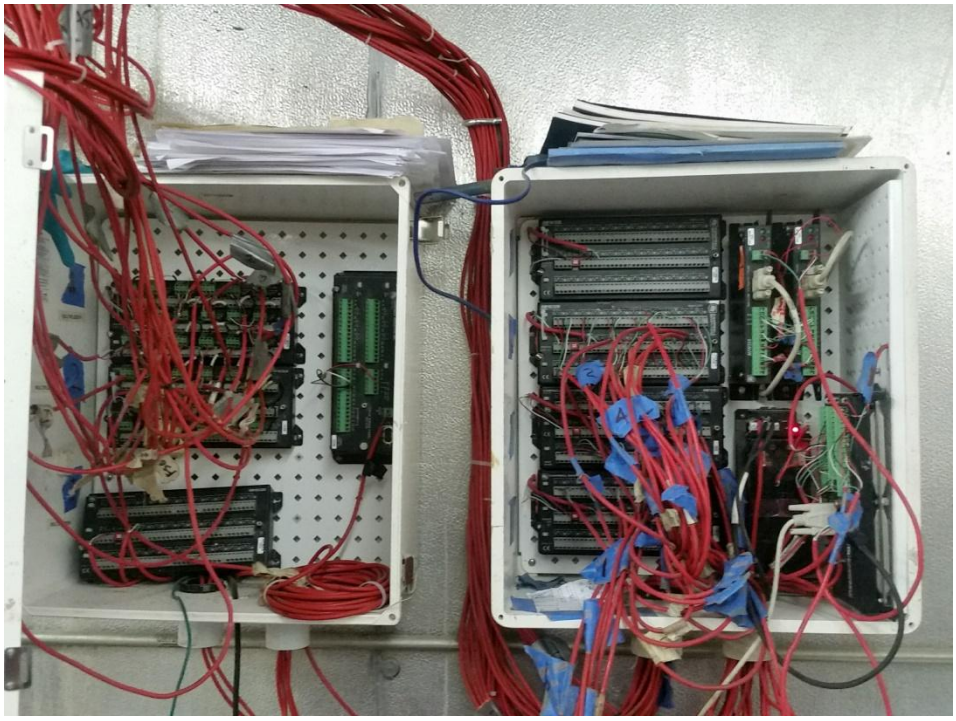

Figure 3.19 Data Logging System

The cracks that form from the restrained shrinkage test are usually small and hard to see with the naked eye. There are various ways to measure crack widths from crack cards to magnifying lenses, but many times they require rough estimating and judgement. To overcome those problems, a digital microscope was used with a variable zoom connected to a computer as shown in Figure 3.20. The program used is called Dinocapture. When a crack is indicated by a jump in strain from either the FSG or VWSG, the microscope is

moved around the ring until a crack shows up on the computer screen. A picture is then taken with the microscope and then the crack can be measured using the tools provided by the program, as long as the zoom on the microscope matches the zoom on the program. An example of one of these pictures with the crack measurement is shown in Figure 3.21. Once a crack forms, pictures are taken periodically to understand the propagation of the crack. At 28 days, the whole ring is analyzed with the microscope to get a full extent of the cracking. The cracking patterns are then mapped out on AutoCAD.

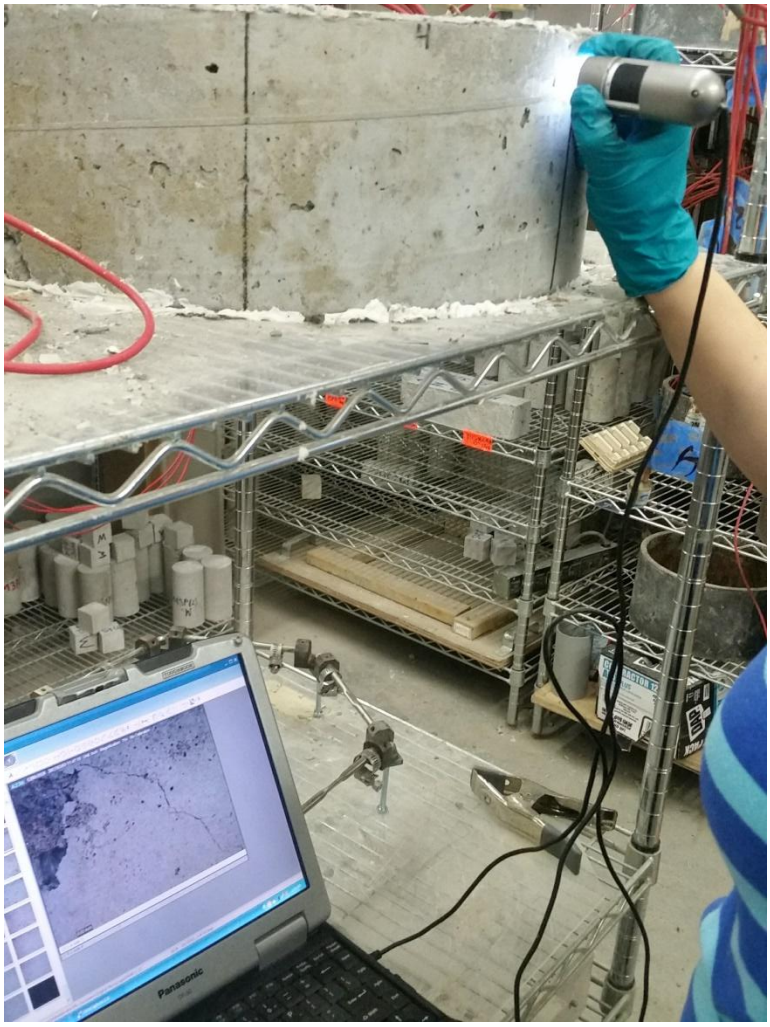

Figure 3.20 Crack Mapping with Digital Microscope

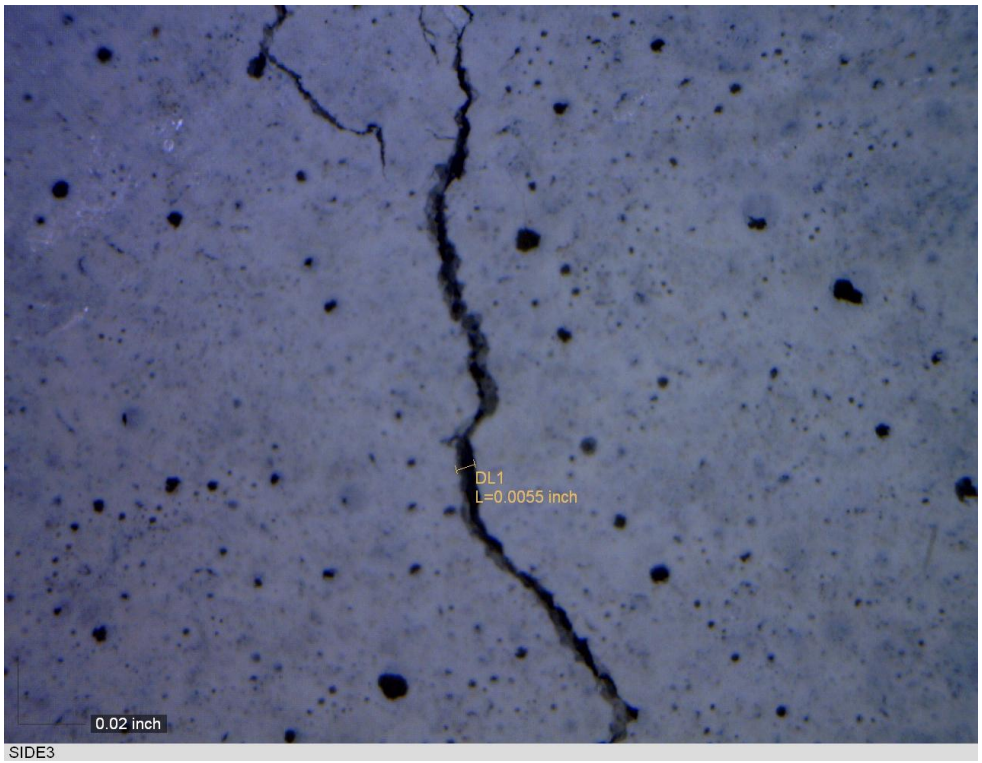

Figure 3.21 Screenshot of Crack Measurement with Dinocapture

CHAPTER IV

4 RESULTS

4.1 Fresh Properties

In set A, the fresh properties of the FRSCC mix were carefully monitored to determine the influence of fiber amount on workability, determine the correct dosage of HRWR to compensate the change in workability, and determine the max fiber amount that would be economical. In set B, the fresh properties were tested again to confirm the results and consistency with set A. The results of fresh properties including, slump test, T20 test, VSI and J-ring test will be presented.

4.1.1 Slump Results

The slump flow according to ASTM C1611 is performed first after all the materials are mixed. Since the control is the same as the control mix of Nassif & Ghanchi, the desired slump is around 24". For the FRSCC mixes, the minimum desired slump for this set of mixes was set at 21". The slump results from set A are presented in Table 4.1 with the same HRWR dosage of 12 oz/cwt.

Table 4.1 Slump Flow

Mix	ST0.00 A	ST0.35 A	ST0.50 A	ST0.65 A	ST0.80 A
Slump, in	23.75	23.625	25	22.25	13

From Table 4.1, it is apparent that low steel fiber content does not affect the flow of the FRSCC compared to the control SCC. There is a steep decrease in flowability from

0.65% to 0.80% by volume. A 13” slump is very low and would most likely not be considered SCC. Attempts were made to increase the slump by adding addition HRWR and remixing. The subsequent results of the added HRWR to the slump are shown in Table 4.2.

Table 4.2 Slump of ST0.80 with Added HRWR

HRWR, oz/cwt	Slump, in
12	13
13	14
14	14.5

After increasing the HRWR amount, the slump could not reach the 21” mark. The mix would have required a lot of extra HRWR and would begin to not become economical as the price of the mix would greatly increase. For this reason, the ST0.80 was not considered for testing in set B as it did not classify as SCC. For set B, the mixes were redone to cast cylinders, shrinkage molds, and rings. To ensure that the mix was consistent the slump test is performed. Since mixes with the same proportions can sometimes vary slightly when redone, some adjustments to HRWR content were done. The slump results of set B are presented in Table 4.3.

Table 4.3 Slump Results of Set B

Mix	ST0.00 B	ST0.35 B	ST0.50 B	ST0.65 B
Slump, in	23.5	24	22	22
HRWR, oz/cwt	12	12	13	13

In set B, the low fiber mixes were able to match the flow of set A with the same amount of HRWR. The mixes with 0.50 and 0.65% by volume needed an extra ounce of HRWR

to achieve the minimum slump. This additional water is accounted for in the mix design tolerances. Overall there is a general trend of decreased workability but the difference in flow is not as severe as the addition of polypropylene fibers as observed by Nassif and Ghanchi, which required additional HRWR with their smallest fiber volume.

4.1.2 T20 Results

During the slump test, the time from when the slump cone is lifted to when the concrete reaches the 20" diameter mark is noted. To ensure stability of the mix and that proper consolidation can occur, the T20 time should be in between 2 and 20 seconds. A lower time constitutes lower viscosity and greater workability. A summary of the T20 times for both sets of mixes are presented in Table 4.4 and plotted in Figure 4.1.

Table 4.4 T20 Times

Mix	ST0.00		ST0.35		ST0.50		ST0.65		ST0.80	
T20, s	A	B	A	B	A	B	A	B	A	B
	5.1	4.3	6.0	4.5	6.4	5.4	6.5	5.4	∞	n/a

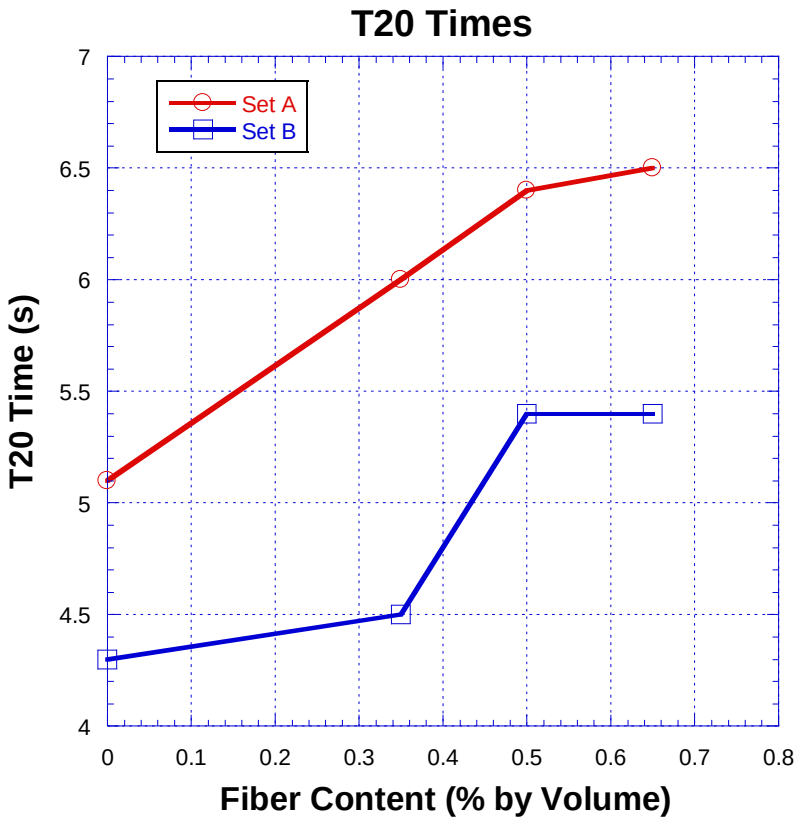

Figure 4.1 T20 Times Vs Fiber Content

As the fiber content increases to about 0.50% by volume, the overall viscosity of the mix consistently decreases and the T20 time rises. After 0.50%, the viscosity seems to level off in both set of mixes. The very high fiber content has less of a negative effect on the flow as the friction energy is already high. In the low fiber mixes, the introduction of steel fibers greatly increases the friction, but that friction increase does not linearly increase with more fibers.

4.1.3 Visual Stability Index (VSI)

The visual stability index is an index to measure the severity of bleeding and segregation of a mix by observing the slump from ASTM C 1611. The VSI for the each mix is presented in Table 4.5.

Table 4.5 VSI Results

Mix	ST0.00		ST0.35		ST0.50		ST0.65		ST0.80	
VSI	A	B	A	B	A	B	A	B	A	B
	0	0	1	0	1	0	1	0	2	n/a

The SCC and FRSCC mixes showed adequate resistance to bleeding and segregation with the exception of ST0.80 which had a VSI index of 2. A VSI index of 2 indicates that additional measures must be taken to reduce segregation. All other mixes had a VSI index of 0 or 1 which is either ideal or acceptable. There is some variance between sets A and B, but overall the mixes pass the VSI test.

4.1.4 J-Ring Results

The J-Ring test is used to determine the passing ability of an SCC mix. The J-ring mimics tightly spaces rebar by allowing the concrete to pass through a circular ring of metal bars. The test is very dependent on the slump of the concrete and is done after the slump test, T20, and VSI. The end slump of the J-ring test is compared to the slump calculated in ASTM C 1611. A small difference in J-ring versus slump indicates the concrete has excellent passing ability since the presence of metal bars does not impede its natural ability to flow. However a large difference, over 2”, in slump indicates inadequate passing ability. The J-ring test was not performed on ST0.80 due to the low slump. The J-ring values and difference in slump are summarized in Table 4.6.

Table 4.6 J-Ring Results

Mix	ST0.00		ST0.35		ST0.50		ST0.65	
	A	B	A	B	A	B	A	B
J-ring, in	22.375	22.75	23.375	23.75	24.5	20.625	19.75	20.625
Slump Difference, in	-1.375	-0.5	-0.25	-0.25	-0.5	-1.375	-2.5	-1.375

The control mix had minimal blocking. The addition of 0.35 and 0.50% fibers had similar or smaller difference in slump and averaged under an inch. This means that there is no significant blocking of the flow. ST0.65 averaged about a 2” difference of flow. Anything beyond 2” is considered extreme blocking. The abundance of large macro fibers did not change the viscosity as much as seen in the T20 results, but problems occur in its ability to pass through barriers. When using high amounts of steel fiber, blocking can become an issue so if there are tight spaces, a maximum of 0.50% fiber amount would be recommended.

4.2 Mechanical Properties

Mechanical properties were tested in both sets of mixes. Set A was tested for compression, tension and modulus at 1,7,28, and 56 days. Set B was tested for compression and tension at 7 and 28 days. Set A is tested with 7 days curing to simulate typical procedure for structures like bridge decks. Set B was limited to one day wet cure to match the curing conditions of the restrained shrinkage rings.

4.2.1 Compressive Test

Compression samples are capped and allowed to dry if they were just demolded or taken out of the water bath. A minimum of two samples are tested until failure and averaged. The results for set A are plotted in psi versus day in Figure 4.2.

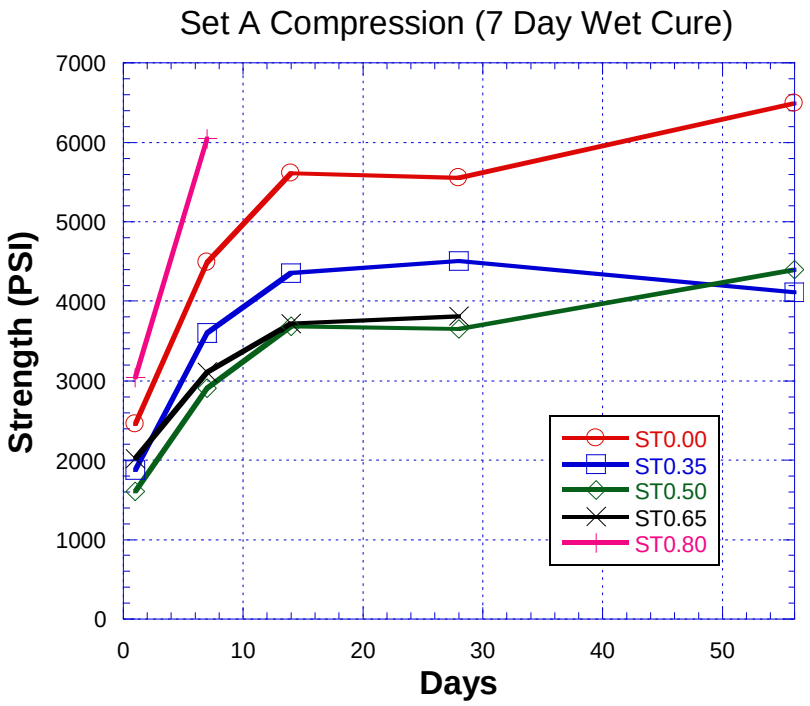

Figure 4.2 Compressive Strength of Set A (7 day cure)

The control mix had the largest compressive strength with the exception of ST 0.80. The strength of the concrete is weakened with the introduction of steel fibers. This is most likely due to the steel fibers disturbing the matrix of the concrete. There is a point around 0.65% fiber that the strength begins to increase as more fiber is added. This is consistent with other research on the use of SFRSCC (Gencel et al. 2011). Set B was tested with one day wet curing, which should yield lower strength as the concrete had less water to use for hydration. The results are shown in Figure 4.3.

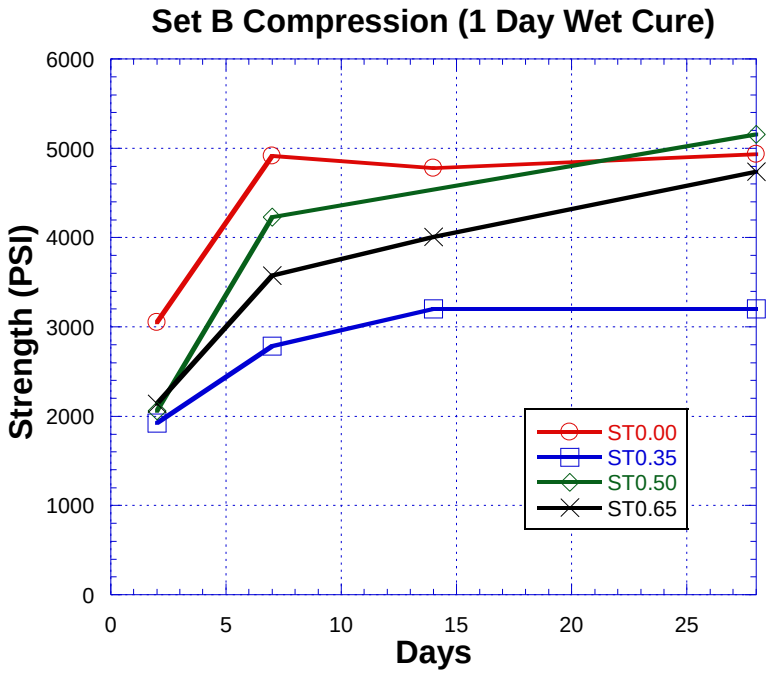

Figure 4.3 Compressive Strength of Set B (1day cure)

In set B, it is apparent that a small fiber volume around 0.35% leads to the largest decrease in compressive strength. ST0.00, ST0.50 and ST0.65 reach similar strength at 28 days. These mixes concrete reached compressive strengths around 5 ksi. Similar to the concrete strengths of set A, compressive strength regains as more fibers are added beyond 0.35%.

4.2.2 Tensile Splitting Test

The tensile strength of the concrete is determined by placing a 4”x8” cylinder horizontally and compressing it until it splits. When the concrete splits in any concrete without fiber or any other type of reinforcement, the concrete splits down the middle and no more load can be applied. With fiber reinforcement, there are sometimes two maximum loads. The first max occurs when loading and there is a drop in load due to the concrete splitting but not breaking. The second is when the concrete fully splits open and

the fibers have no pull left. The true tensile stress and the stress that will be recorded for this test is the first max load. The tensile strengths for set A and B are shown in Figure 4.4 and Figure 4.5.

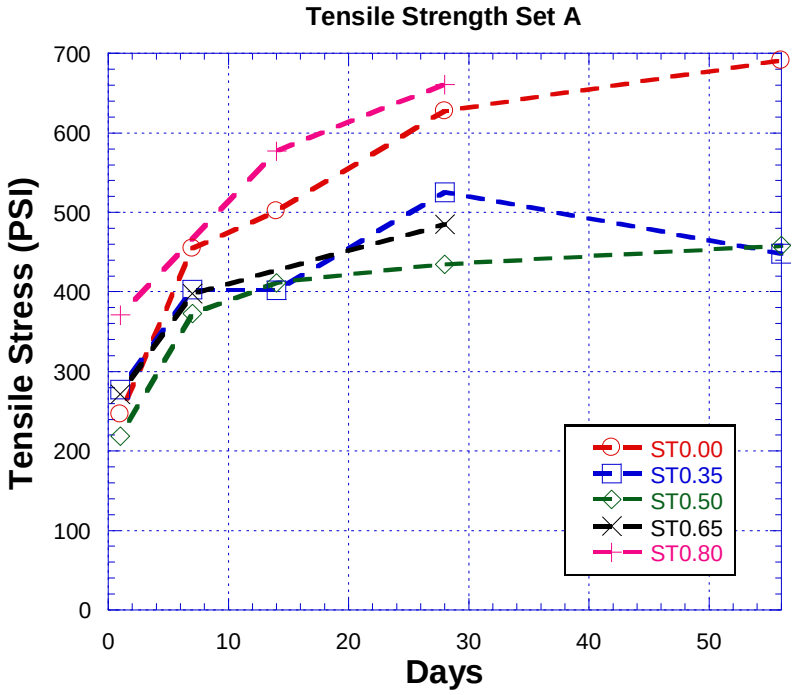

Figure 4.4 Tensile Strength Set A (7day curing)

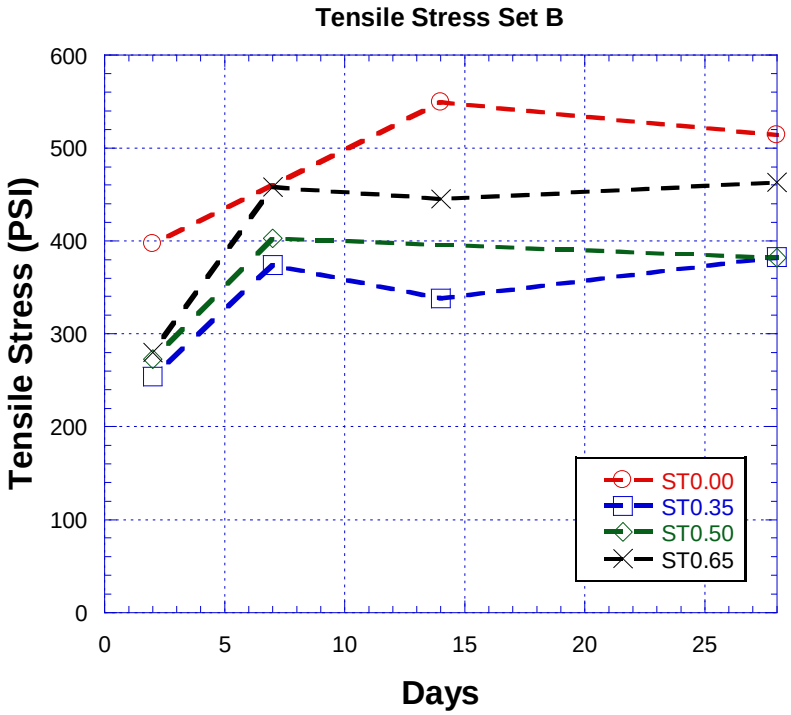

Figure 4.5 Tensile Strength Set B (1 day wet cure)

The tensile stresses in set A are about 10% higher than set B. The tensile splitting stress is lower in the mixes which have fibers. In both sets A and B the control mix has the higher with the exception of ST0.80 in set A. The tensile results are consistent with the compression results with the fibers seeming to have a negative effect on strength with small and medium amounts of steel fiber. The disturbance of the concretes matrix causes the concrete to split at a lower stress. In ST0.80, the higher tensile strength may be a result of the very large concentration of fibers that prevent the majority of any microcracks to force the first split in the concrete, allowing the higher tensile stress shown in the results. However, there is clear difference after the concrete cracks that the data cannot show. Instead of the entire specimen splitting apart, the fibers keep the concrete intact and allow the specimen to deform and take more tensile load. The deformed shape of an FRSCC specimen after failure can be seen in Figure 4.6.

Figure 4.6 Deformation of FRSCC Under Tensile Splitting

4.2.3 Elastic Modulus Results

Elastic modulus tests were performed on set A after the 7 day wet cure. Before the test, compression testing was done to determine the maximum load the samples can endure during the test. Each sample was tested twice and a minimum of two samples were tested. Knowing the elastic modulus and tensile strength of the specimen, the cracking strain of the concrete can be calculated using Equation 4.1.

$$\text{Cracking Strain } (\mu\varepsilon) = \frac{Tensile\ Strength}{Elastic\ Modulus} \tag{4.1}$$

The cracking strain is the expected strain that the concrete can take before it begins to crack. This value is important for the concretes performance under restrained shrinkage. The elastic modulus will be assumed to be the same for set A and B. Table 4.7 includes

the elastic modulus results as well as the cracking strain using the 28 day tensile strength results from set B and equation 4.1.

Table 4.7 Elastic Modulus and Cracking Strain

Mix	ST0.00	ST0.35	ST0.50	ST0.65
Elastic Modulus, ksi (% diff from control)	3892 (0%)	3863 (-0.7%)	3688 (-5.2%)	3592 (-7.7%)
28 Day Tensile Strength , psi (% diff from control)	514 (0%)	383 (-25.5%)	382 (-25.5%)	463 (-9.9%)
Cracking Strain, (με) (% diff from control)	132 (0%)	99 (-25.0%)	104 (-21.2%)	129 (-2.3%)

In Table 4.7, there is a general trend of a lower elastic modulus with increasing fiber content. The cracking strain calculated sharply decreases with the introduction 0.35% fibers but then quickly rises as a result of the combination of increased tensile strength and lower elastic modulus. The negative effects fibers have on the strength are compensated with increasing cracking strain.

4.3 Free Shrinkage

A minimum of 2 free shrinkage samples were measured to see the influence of fibers on free shrinkage. For this study, a length comparator was used to measure the change in volume to the accuracy of .0001 inches. Each sample is checked 3 times and converted to microstrain. The average microstrain is tracked for 91 days. Beyond 91 days, free shrinkage is minimal although theoretically, shrinkage can continue beyond. The results for the free shrinkage of the mixes in set B are shown in Figure 4.7.

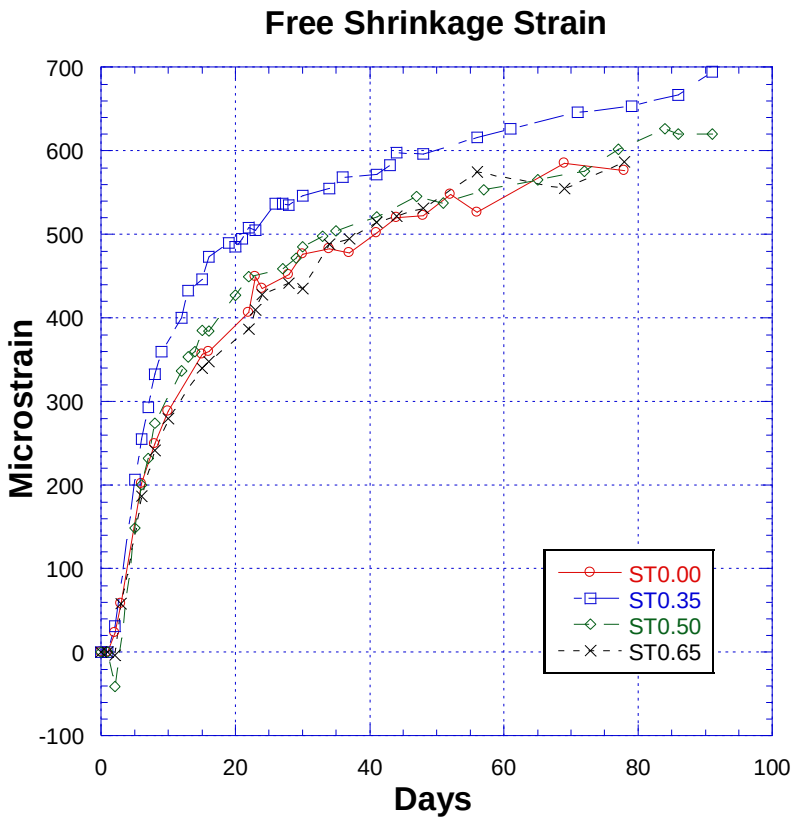

Figure 4.7 Free Shrinkage Strain

The introduction of steel fibers does not seem to greatly affect the free shrinkage. ST0.35 did show about a 15% higher ultimate shrinkage than the other mixes. The mix without fibers, ST0.50, and ST0.65 showed very similar trends in shrinkage rates throughout the entire 91 days. During the first day, there are signs of swelling as the shrinkage dips below 0 microstrain. This is due to the samples being in the water bath. When the sample is fully submerged, the drying and autogenous shrinkage is none to minimal.

4.4 Restrained Shrinkage

When the restrained shrinkage rings, both ASTM and AASHTO, are demolded at 24 hours, all strain gauges must be connected to the data collection system and zeroed out. The zero time for this test will the time once the molds were transferred to the

environmental chamber immediately after casting. For both rings, circumferential drying is guaranteed by sealing the top portions of the concrete by melting paraffin wax and allowing it to dry and cover all the concrete. To prevent evaporation from the bottom, the concrete is caulked on the bottom. For each mix, 1 ASTM and 2 AASHTO rings are casted at the same time and analyzed for up to 28 days.

4.4.1 ASTM Ring Results

For the ASTM ring test, cracking is expected to occur quickly so the ring is checked for signs of cracking frequently during the first week of the test. The data is checked for signs of cracking by observing any jumps in the steel strain. Large jumps indicate a relaxation meaning that the concrete cracked and is free to shrink with less restraint and hence less strain on the steel. The ring is then observed for viewable signs of cracking by eye or digital microscope. When the crack is spotted, the time, a picture, and crack width are noted and tracked until 28 days when the test is terminated. At 28 days the whole ring was crack mapped for appearance of any small additional cracks. The results of the ASTM ring for each mix are presented in the next few sections.

4.4.1.1 ST0.00 ASTM

The restrained shrinkage test for the control mix had 4 FSGs and no VWSGs. The strain graph is shown in Figure 4.8. During the test, FSG 2 stopped working and was neglected in the results. At day 6.4, all FSGs show a large jump in strain indicating a crack. The ring was then observed and it showed a full length crack near the area of FSG 1 and a crack near FSG 2 on the opposite side. The max strain at which the ring endured before cracking was about 78 microstrain. At 28 days the max crack width observed in the 2

cracks are 0.0231". The crack mapping showing the relative size of the total cracks and crack widths measured using a digital microscope are shown in Figure 4.12.

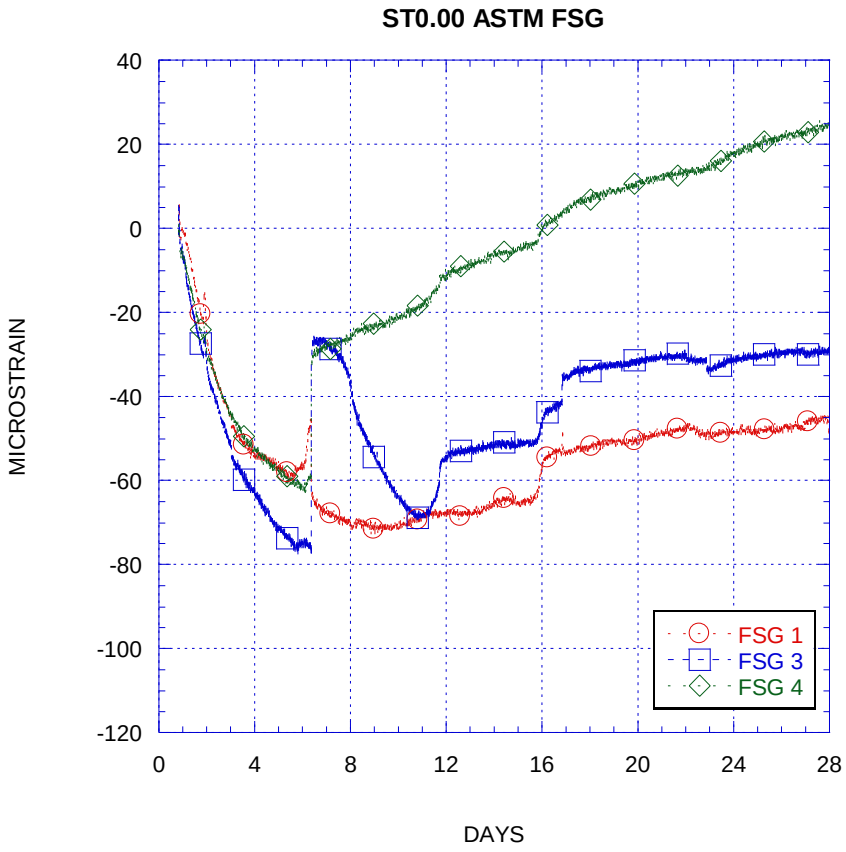

Figure 4.8 ST0.00 ASTM FSG Data

4.4.1.2 ST0.35 ASTM

The next mix has 0.35% fiber which had the lowest strength, highest free shrinkage and lowest cracking strain of all the mixes. The strain graph is shown in Figure 4.9. At day 7.5, all FSGs show a large jump in strain indicating a crack. The ring was then observed and it showed a full length crack near the area of FSG 1. The max strain at which the ring endured before cracking was about 95 microstrain. Two days later, a second crack appeared on the opposite side. At 28 days the max crack width observed in the 2 cracks

are 0.0089". This ring cracked around the same time as the control mix but saw a sizeable decrease in crack width. The crack mapping showing the relative size of the total cracks and crack widths measured using a digital microscope are shown in Figure 4.13.

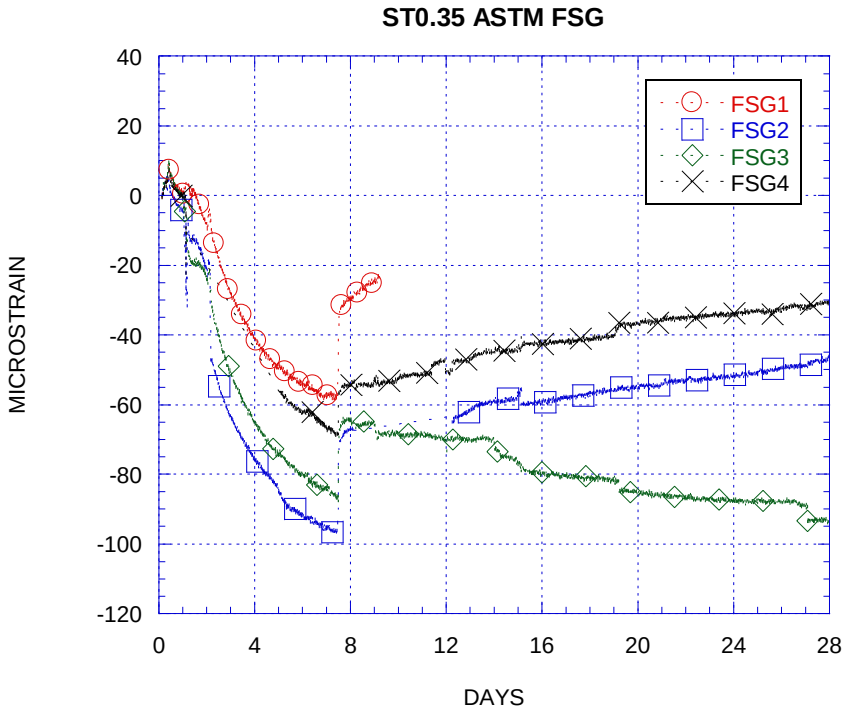

Figure 4.9 ST0.35 ASTM FSG Data

4.4.1.3 ST0.50 ASTM

The next mix has 0.50% fiber which had higher strength, lower free shrinkage and higher cracking strain than ST0.35. The strain graph is shown in Figure 4.10. FSG 2 was determined to be unreliable and is neglected from the graph. At day 6.8, all FSGs started to no longer increase in strain. This could be an indication of a microcrack forming near the ring. The ring was then observed and it showed a small crack. At day 8.1, the crack fully propagated the full length near the area of FSG 1. The max strain at which the ring endured before cracking was about 53 microstrain. Around the same time of the fully

propagated crack, a second crack appeared on the opposite side in between FSG 2 and 3. At 28 days the max crack width observed in the 2 cracks are 0.0062". This ring cracked around the same time as the control mix but the crack did not fully propagate until day 8.1. The crack mapping showing the relative size of the total cracks and crack widths measured using a digital microscope are shown in Figure 4.14.

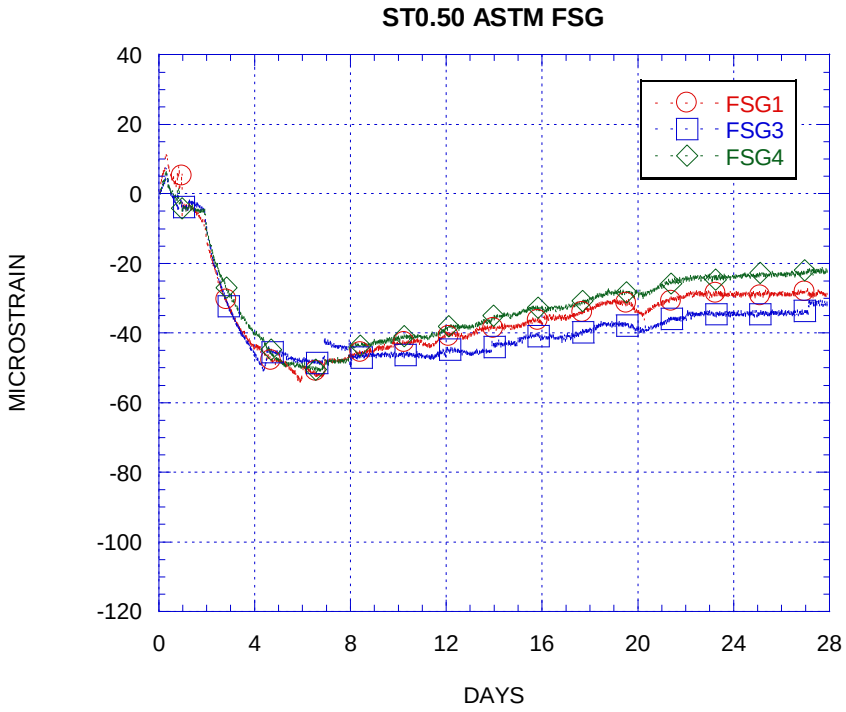

Figure 4.10 ST0.50 ASTM FSG Data

4.4.1.4 ST0.65 ASTM

The next mix has 0.65% fiber which is the highest fiber amount used in the restrained shrinkage testing and had the highest cracking strain of the FRSCC mixes. The strain graph is shown in Figure 4.11. FSG 2 was determined to be unreliable and is neglected from the graph. At day 4.8, all FSGs started to no longer increase in strain and show signs of relaxing. This could be an indication of a microcrack forming near the ring. The ring was then observed and it showed a small crack near FSG 4. The crack was small and took a couple days to be large enough to be seen with the naked eye. At day 9.0, the crack fully propagated the full length near the area of FSG 4. The max strain at which the ring endured before initial cracking was about 48 microstrain. However, the ring continued to take more strain as the fibers helped to keep the ring intact. At day 20 the strain maxed out at 62 microstrain and another crack formed near FSG 2. At 28 days the max crack width observed in the cracks are 0.0062” which is similar to ST0.50. This ring cracked the earliest of all the rings but the cracks took the longest to fully propagate at day 9.0. The crack mapping showing the relative size of the total cracks and crack widths measured using a digital microscope are shown in Figure 4.15.

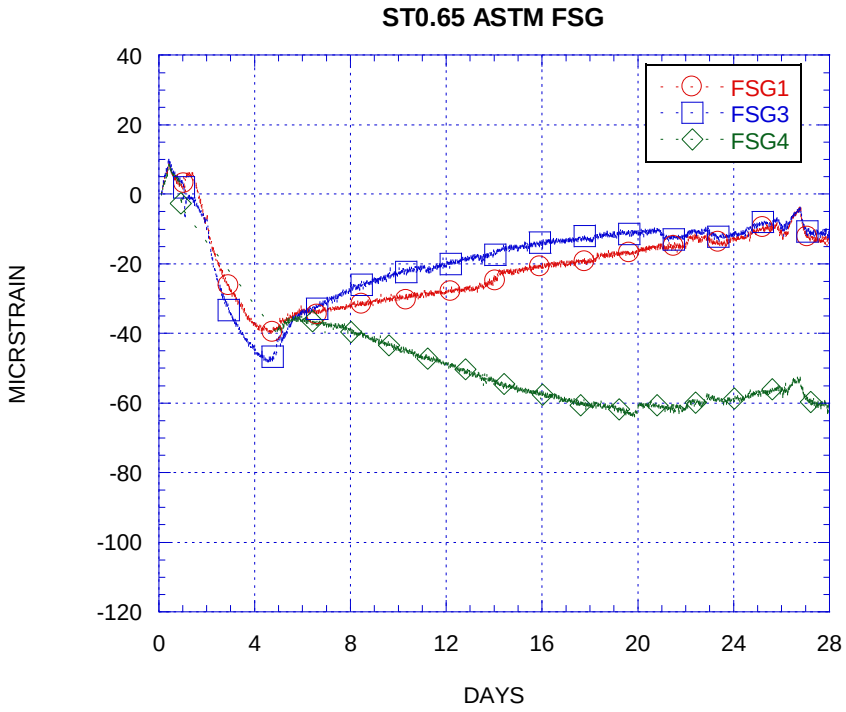

Figure 4.11 ST0.65 ASTM FSG Data

4.4.1.5 ASTM Ring Summary

The results of the ASTM ring test can be summarized in Table 4.8. The control mix and ST0.35 cracked at 6.4 and 7.5 days respectfully. When these rings cracked, there was no delay in creating a fully propagated crack. In ST 0.50 and ST0.65 there was a delay of a couple days for the initial crack to fully propagate the full height of the ring. Based on initial days to cracking, increasing fiber content seems to accelerate cracking, but when looking at the days to full cracking, there is a clear improvement in cracking resistance. A big improvement came in the reduction of maximum crack width with lowest fiber amount reducing the crack width from .0231" to .0089". Another way to observe the cracking resistance is by looking at the total cracking area by adding together all the crack widths with their respective lengths in terms of area. When this area is divided by

the circumferential area, the cracking percentage can be calculated. A large decrease in total crack area was apparent with the smallest fiber amount and continued to decrease with increasing amounts. The reduction in crack widths and crack area were similar and consistent in terms of percent difference from the control mix. The full extent of cracking in all the mixes including the crack widths can be seen in the crack mapping shown in Figure 4.12, Figure 4.13, Figure 4.14, and Figure 4.15.

Table 4.8 Summary of ASTM Ring Results

Mix	ST0.00	ST0.35	ST0.50	ST0.65
Days to first crack (%diff from ST0.00)	6.4 (0%)	7.5 (+17%)	6.8 (+6%)	4.8 (-25%)
Days to full crack (%diff from ST0.00)	6.4 (0%)	7.5 (+17%)	8.1 (+27%)	9.0 (+40%)
Max crack width, in (%diff from ST0.00)	.0231 (0%)	.0089 (-61%)	.0062 (-73%)	.0062 (-73%)
Cracking Area, % (%diff from ST0.00)	.064 (0%)	.020 (-68%)	.017 (-73%)	.018 (-71%)

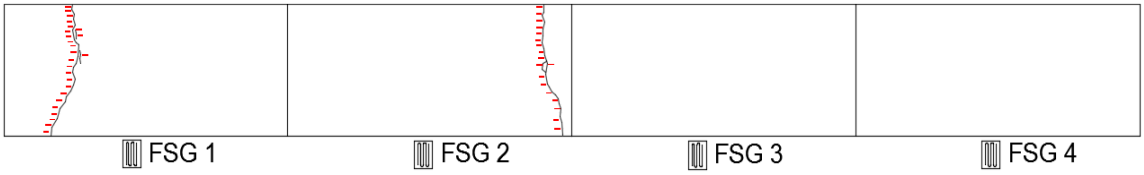

Figure 4.12 ST0.00 28 Day Crack Map

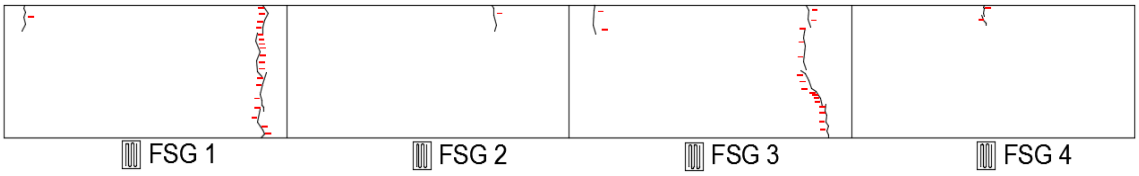

Figure 4.13 ST0.35 28 Day Crack Map

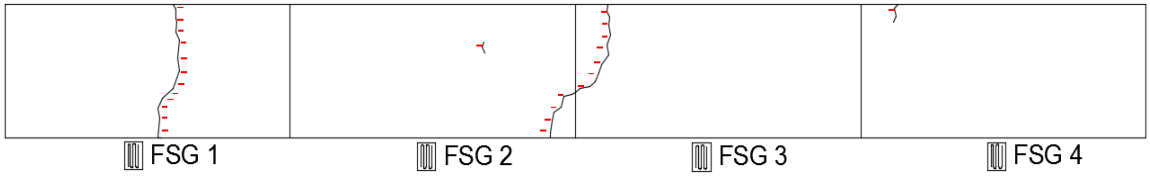

Figure 4.14 ST0.50 28 Day Crack Map

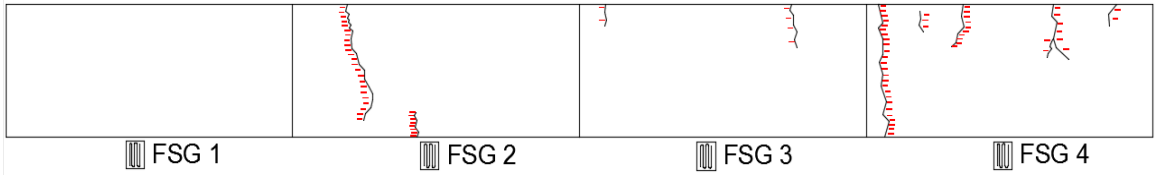

Figure 4.15 ST0.65 28 Day Crack Map

4.4.2 AASHTO Ring Results

For the AASHTO ring test, cracking is expected to occur slower than the AASHTO ring due to the increased concrete thickness and smaller ring diameter. The checked for signs of cracking more frequently during the second and third week of the test. The data is checked for signs of cracking by observing any jumps in the FSG strain and also in jumps in the VWSG data. Large jumps in the FSG indicate a relaxation meaning that the concrete cracked and is free to shrink with less restraint and hence less strain on the steel. A jump in the VWSG data means that over the span of the gauge, a crack in the concrete cause the gauge to lengthen. After the crack forms, the VWSG in the section of the crack will continue to read a higher strain as it is effectively measuring the crack widen instead of the strain in the concrete. The ring is then observed for viewable signs of cracking by eye or digital microscope. The VWSG will usually give the section at which the crack most likely is at. When the crack is spotted, the time, a picture, and crack width are noted and tracked until 28 days when the test is terminated. At 28 days the whole ring was

crack mapped for appearance of any small additional cracks. The results of the AASHTO rings for each mix are presented in the next few sections.

4.4.2.1 ST0.00 AASHTO Ring

The control mix with no fiber had one sample that cracked (ring B) and another that did not (ring A). The cracked ring (ring B) cracked at 20.6 days according to both VWSG and FSG data. This was confirmed with visual inspection with a full crack on two sides (section 2 and section 6). After 21 days, the cracks opened up and put the 2 associated VWSGs in tension while the rest became in tension. Prior to the crack, strains in the concrete were low in most sections with the exception of section 5 and 6 (one in tension one in compression). This can indicated the compression in section 5 is pulling section 6 into tension up until a breaking point at 21 days. The FSG data of both rings are shown in Figure 4.16 and the VWSG data are shown in Figure 4.17. The 28 day crack mapping is shown in Figure 4.18 andFigure 4.19.

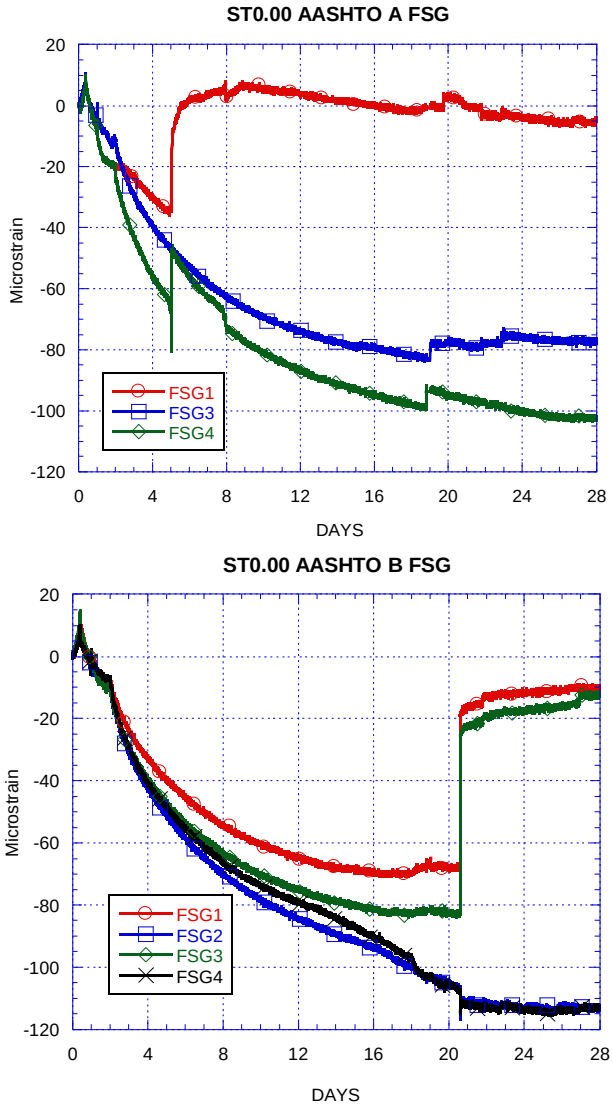

Figure 4.16 ST0.00 AASHTO A & B FSG Data

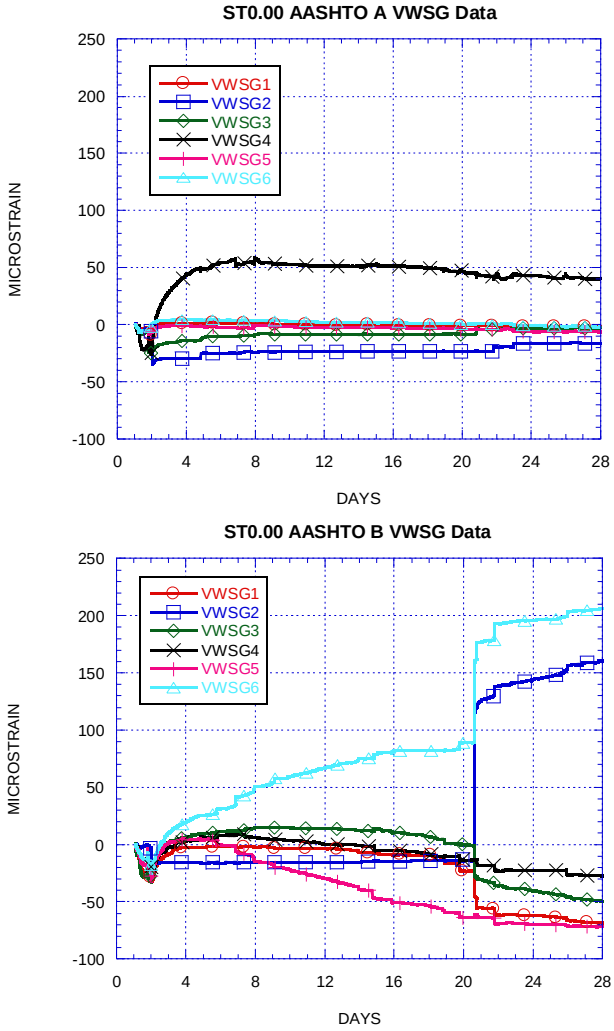

Figure 4.17 ST0.00 AASHTO A & B VWSG Data

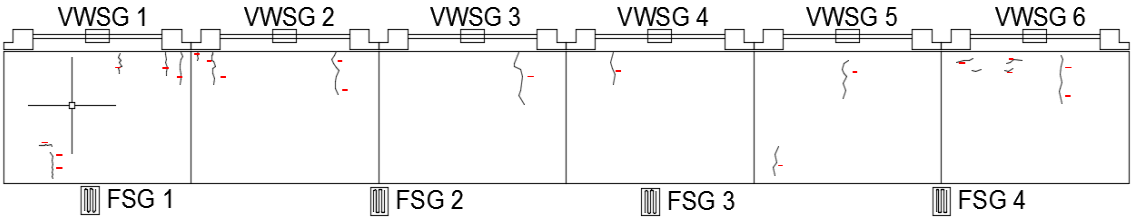

Figure 4.18 28 Day Crack Map ST0.00 A

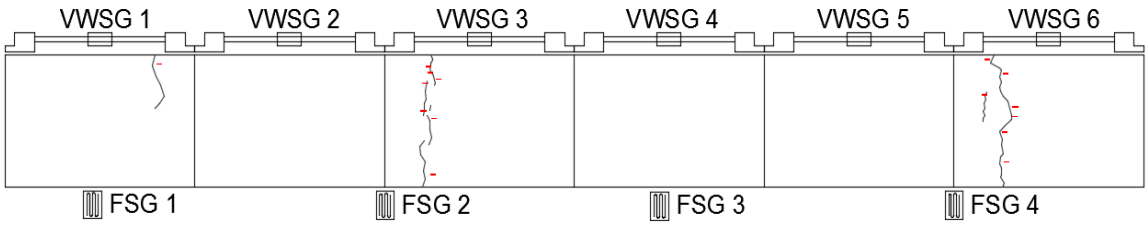

Figure 4.19 28 Day Crack Map ST0.00 B

4.4.2.2 ST0.35 AASHTO Ring

The addition of fibers affected the crack tendency and strain data when compared to the control ring. The graphs for the FSGs of both rings can be seen in Figure 4.20 and the graphs for the VWSGs can be seen in Figure 4.21. The 28 day crack mapping is shown in Figure 4.22 andFigure 4.23. Again, one ring fully cracked (ring A) and the other ring did not fully crack (ring B). ST0.35 A did crack earlier (days 9.6) but the crack was small and not visible. It is known that a crack formed due to the jumps in the FSGs and the runaway tension that section 6 was in after day 10. After the microcrack, the steel ring continued to take stress. This is most likely due to the fact that the fibers have kept the ring together and did not let the crack propagate through the whole thickness of the ring. As shrinkage continued, the crack became visual and fully propagated at around day 22. This was consistent with both FSG and VWSG data with another jump in the data and section 6 rising in tension. We do see a similarity in the relationship between section 4, 5, and 6 that was seen in the control ring (section 5 and 6). Prior to the initial crack, sections 4 and 5 went from slight tension into compression until finally section 6 cracked. Crack map data at 28 days confirms the crack at section 6. When the crack fully propagated, the rest of the VWSGs were put into compression as section 6 had the crack which allowed it to open up. After this full crack, the FSGs indicated no additional stress in the steel.

Ring B had no full visible cracking. In between 6 and 12 days, FSG 2 saw a decrease and then an increase in strain over time, but after no cracking was found, it was determined to be a temporary malfunction. There were no big jumps in the FSG data over the 28 days to indicate cracking. At day 28 the strain in the steel seemed to be reaching a level point which meant that the ring was close to cracking. VWSG 6 showed signs of opening up as the strain were increasing. The 28 day crack mapping shown in Figure 4.22 and Figure 4.23 confirmed a crack in that area in addition to small cracks randomly assorted throughout the rest of the ring.

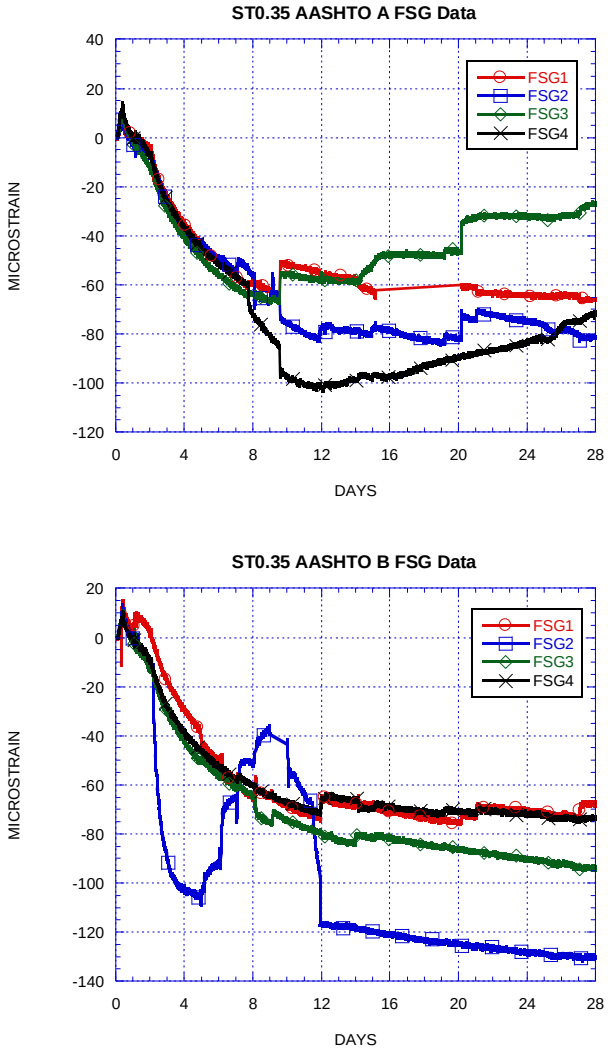

Figure 4.20 ST0.35 AASHTO A & B FSG Data

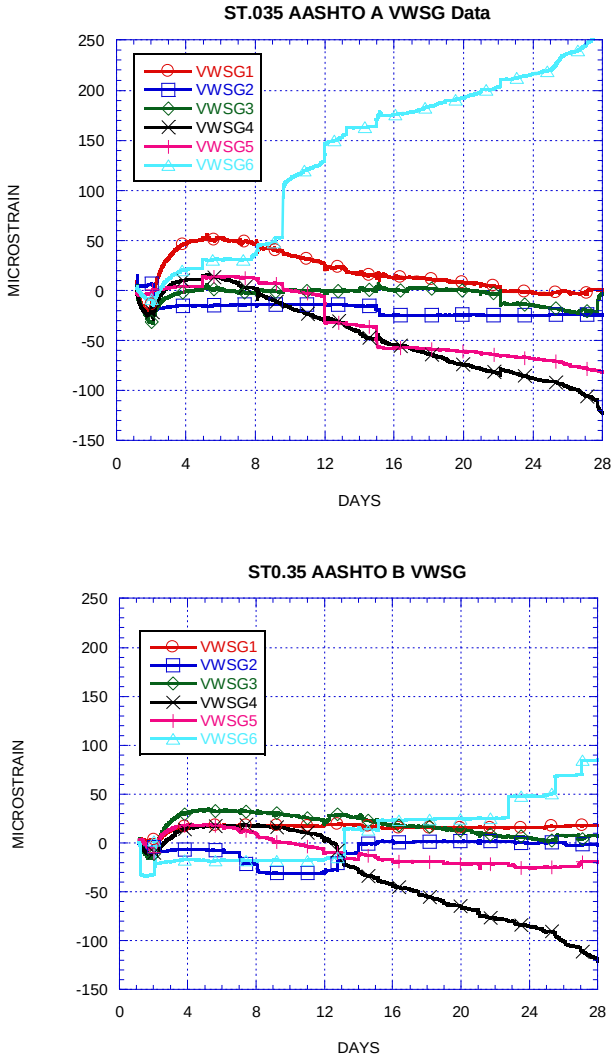

Figure 4.21 ST0.35 AASHTO A & B VWSG Data

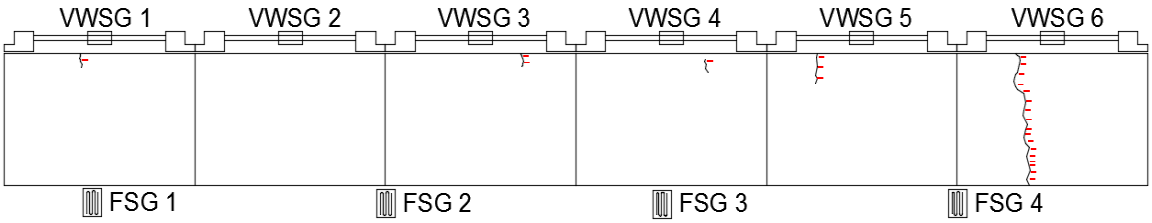

Figure 4.22 28 Day Crack Map ST0.35 A

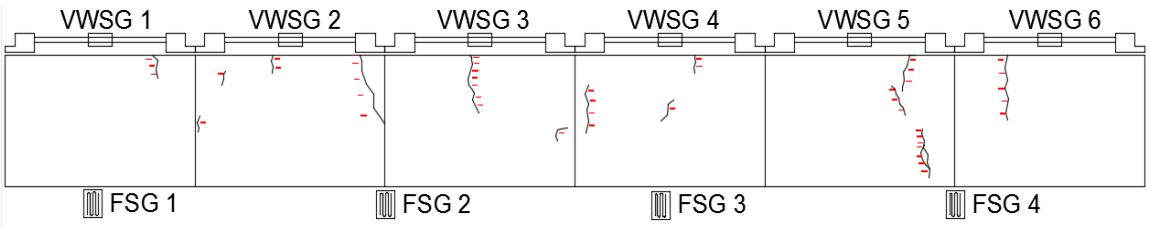

Figure 4.23 28 Day Crack Map ST0.35 B

4.4.2.3 ST0.50 AASHTO Ring

ST0.50 once again had one ring crack (ring A) and the other ring not crack (ring B).The graphs for the FSGs of both rings can be seen in Figure 4.24 and the graphs for the VWSGs can be seen in Figure 4.25. The 28 day crack mapping is shown in Figure 4.26 andFigure 4.27In ring A, there was a small jump in strain around day 13 but no crack was found. This was a most likely a micro crack that was intercepted by the steel fibers since the ring continued to endure strain for another 7 days. At 20 days, all FSGs jumped indicating there was a large crack that formed. This was consistent with the VWSG data which saw large jumps in strain in VWSG 1 and 4. A visual inspection saw full propagated cracks in sections 1 and 4.

In ring B there was no sign of cracking in the FSG data up until 28 days. Based on the slope of the strain curve, the strain was a couple days from leveling out which means it had good cracking resistance. The VWSG for ring B showed almost no points where the strain greatly increased indicating the presence of a large crack. Around day 26, VWSG 1 started to increase in strain. When the crack map at 28 days was performed the only crack found was in section 1. This shows the effectiveness of the VWSG to predict a crack that the FSG in the steel sometimes can't catch.

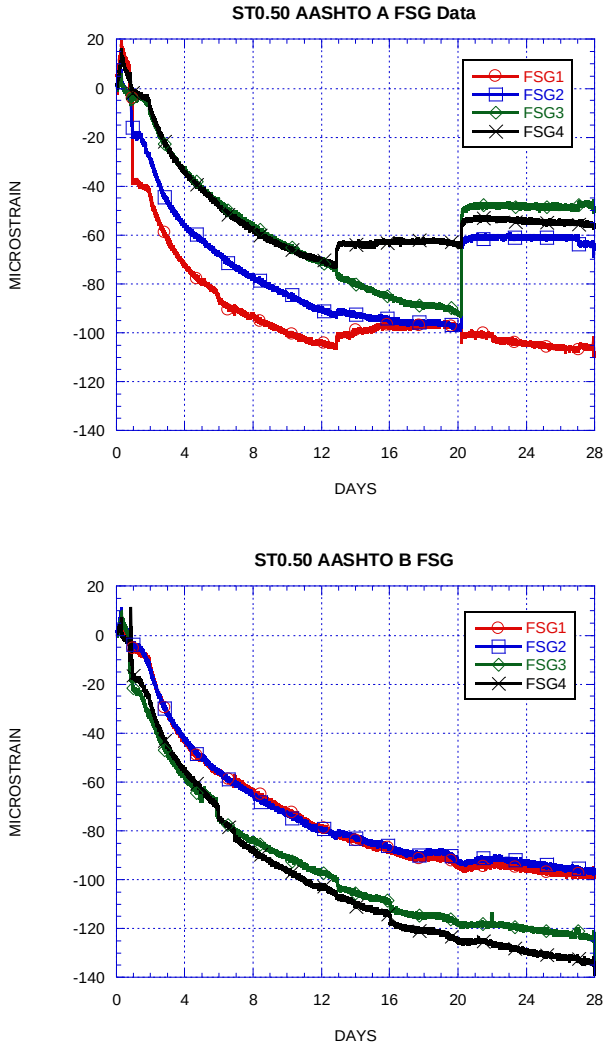

Figure 4.24 ST0.50 AASHTO A & B FSG Data

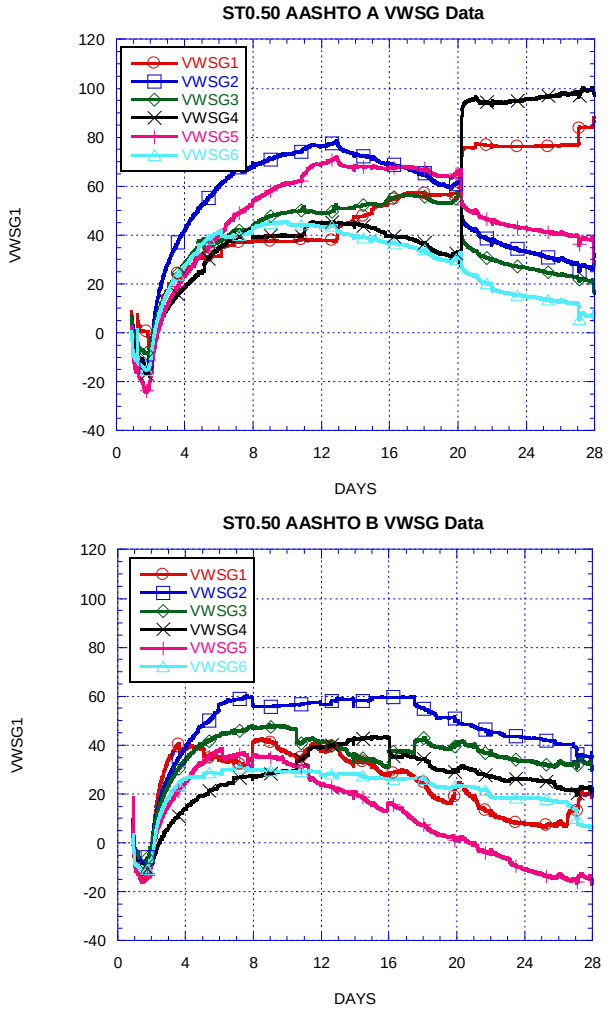

Figure 4.25 ST0.50 AASHTO A & B VWSG Data

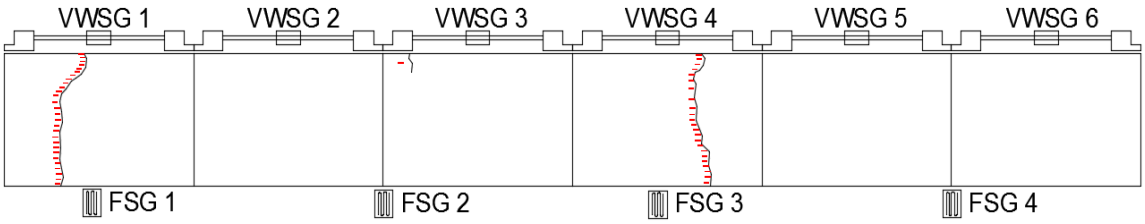

Figure 4.26 28 Day Crack Map ST0.50 A

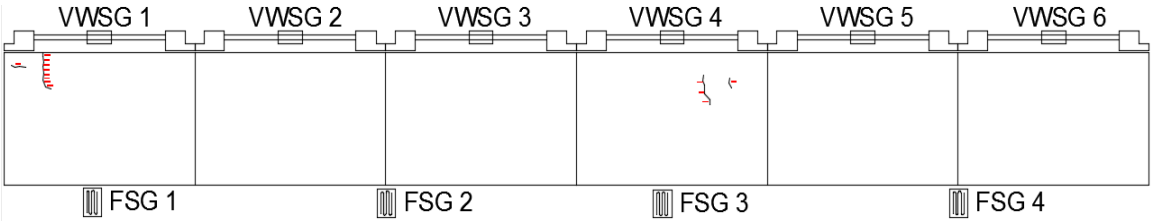

Figure 4.27 28 Day Crack Map ST0.50 B

4.4.2.4 ST0.65 AASHTO Ring

ST0.65 is the highest fiber content used in this study. It has the highest cracking strain of 3 FRSCC mixes but may not have the passing ability for some situations. Based on the mechanical properties and the trends of ST0.35 and ST0.50, there should be less severe cracking during the AASHTO ring test. In the ASTM ring test, ST0.65 showed a superior ability to delay cracking from fully propagating. The graphs for the FSGs of both rings can be seen in Figure 4.28 and the graphs for the VWSGs can be seen in Figure 4.29. The 28 day crack mapping is shown in Figure 4.30 and Figure 4.31. In this test both rings (ring A and ring B) did not have any large cracks. In Ring A, FSG 2 was deemed unreliable and FSG 3 began to show a great increase in strain around day 22. After inspection it was seen that the wire was put into tension and was giving unreliable readings after that time. It is apparent that no jumps or relaxation was occurring. In both rings A and B, the strain was continuing to decrease in at least two of the FSGs. This indicates that the concrete still maintained a high degree of rigidity to take more stress. In the VWSGs there were also no jumps with the exception of VWSG 6 in ring A. Although not a jump, the data indicates that stress distribution was not evenly distributed as the only section in tension in the second half of the test was VWSG 6. From this data it is easy to predict that over time, if a crack occurs it will be in that section as all the other sections were in compression. The full crack mapping confirms a small crack in section

6. The high fiber content helps to block these cracks from propagating. In ring B, crack mapping showed multiple small cracks but none propagating more than a third of the whole height of the ring.

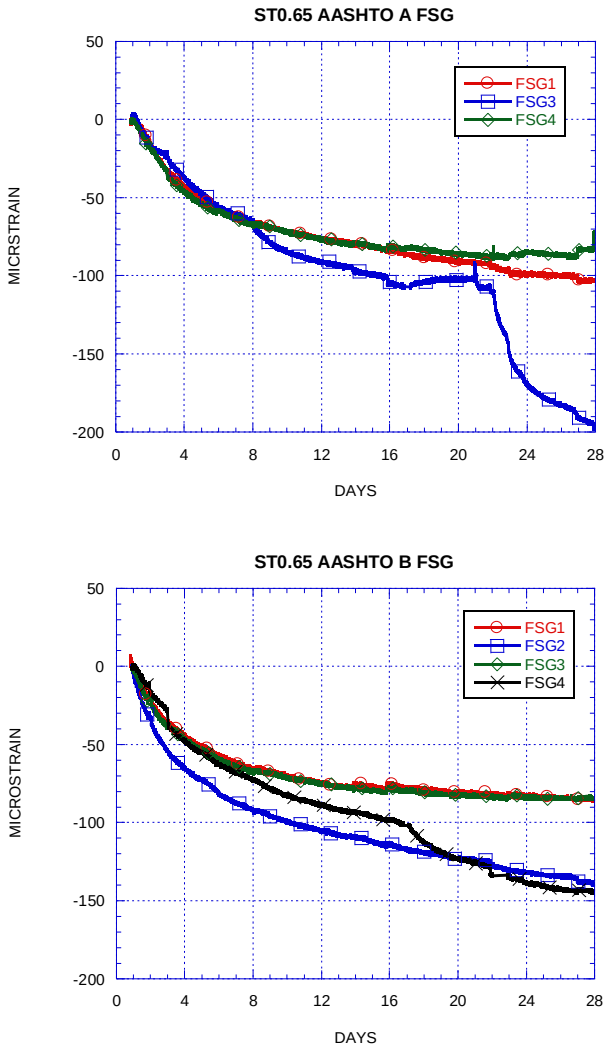

Figure 4.28 ST0.65 AASHTO A & B FSG Data

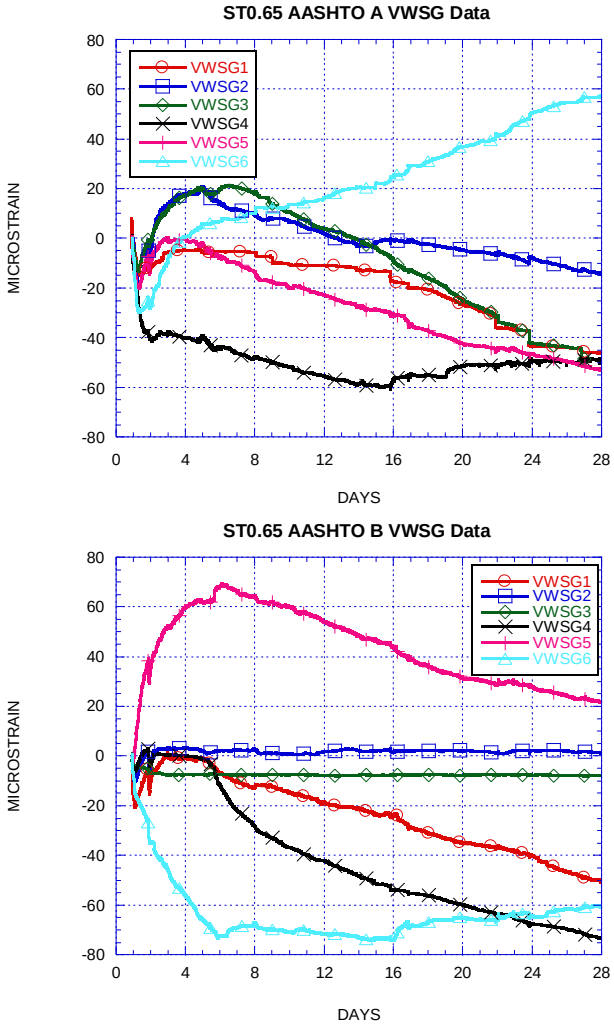

Figure 4.29 ST0.65 AASHTO A & B VWSG Data

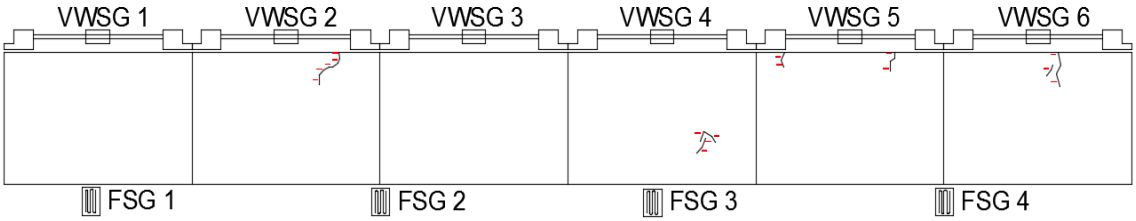

Figure 4.30 28 Day Crack Map ST0.65 A

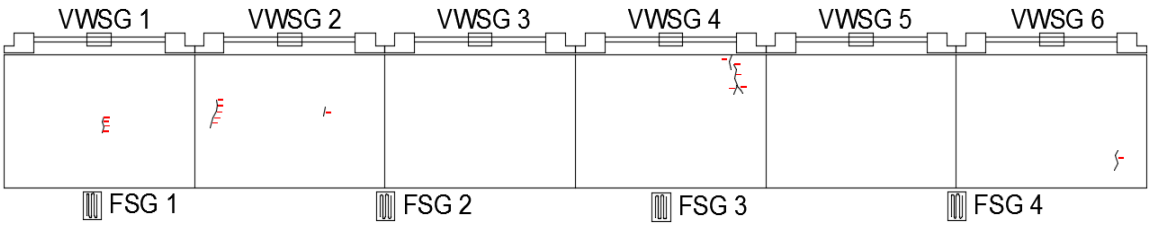

Figure 4.31 28 Day Crack Map ST0.65 B

4.4.2.5 AASHTO Ring Summary

This section will summarize the AASHTO ring test by looking at a number of different observations. The first observation will be the days to first cracking. To determine this, jumps in the data indicate a microcrack or large crack that formed that leads to a slight relaxation in the steel. In the control mix this first crack was inconsistent, with a jump in the data at 4.8 days which never lead to a full crack. It is possible that this crack formed early but as the concrete cured, the stronger concrete isolated the small internal crack. The other control ring did not have any jumps until day 20.6. ST0.35 had microcracks form at days 9 and 13 and each FRSCC mix afterwards took longer to have a first crack form with ST0.50 matching the control mix at 20.5 days and ST0.65 not cracking until 28 days.

The next observation will be the days to full cracking. A full crack will be defined as a crack that propagates the entire height of the ring. Of the 8 total rings casted, only 3 had fully propagated cracks. Each mix had one except ST0.65 which had no fully propagated cracks. ST0.00, ST0.35, and ST0.50 had a ring that fully propagated at 20.6, 21, and 20.5 days respectfully. From this we can see the low fiber amounts don't delay the time to fully propagated cracks, but with ST0.65 not having a fully propagated crack, there are indications that high fiber amounts can delay full cracking. Another way to observe the

fibers ability to prevent propagation, is to see the percent propagation of the cracks at 28 days. Percent propagation will be defined by the longest length of the crack over the height of the ring. By understanding the percent propagation, you can see how close the crack was to full propagation and infer how well the concrete is at preventing propagation. In both rings for ST0.00 and ST0.35, there was at least one crack with at least 45% propagated. In ST0.50 and ST0.65 no cracks were more than 25% propagated with the exception of the one full crack in ST0.50.

The last observation to summarize is the max crack width and total crack area. Fibers have been shown to reduce crack widths and this study confirms this. With the exception of ST0.35 which had similar crack widths, ST0.50 reduced max crack widths up to 25% and ST0.65 reduced max crack widths by over 50% compared to the largest crack width in both control rings. The cracking area was the largest in ST0.00 and ST0.35 which also both contained the largest crack widths and highest % propagation. As more steel was added the crack areas began to decrease with ST0.50 having about a 50% decrease in crack area and ST0.65 having about a 75% decrease in crack area.

Table 4.9 AASHTO Ring Summary

Ring	**ST0.00**		**ST0.35**		**ST0.50**		**ST0.65**	
	A	B	A	B	A	B	A	B
Days to first crack	20.6	4.8	9	13	20.5	20.5	28	28
Days to full crack	20.6	n/a	21	n/a	20.5	n/a	n/a	n/a
% crack propagation	100%	45%	100%	75%	100%	25%	20%	25%
Max crack width @28day	.0059”	.0022”	.0067”	.0028”	.0045”	.0022”	.0028”	.0022”

Cracking area, %	0.0065	0.0197	0.0103	0.0189	0.0124	0.0015	0.0044	0.0032

CHAPTER V

5 SUMMARY AND CONCLUSIONS

5.1 Conclusions

The focus of this study was to analyze the cracking behavior of an economical SCC mix with the addition of crimped steel fiber. The mix design, taken from an investigation of FRSCC by the Virginia Transportation Board and used by Nassif and Ghanchi in their investigation with the use of polypropylene fibers, is both economic and highly workable. The materials are locally available and slag was used to partially replace the Portland Type I cement. Using the same mix design as Nassif and Ghanchi, a comparison between the advantages of steel versus polypropylene fibers can be made. The properties primarily tested for in this study are the fresh properties including workability and passing ability, mechanical properties including strength and modulus, and shrinkage properties including free and restrained shrinkage.

This study looks to draw conclusions between the mixes used in this study, and the use of ASTM rings versus AASHTO rings with the VWSG modification.

1. *Workability*- The addition of steel fibers negatively affected workability at high fiber contents over 0.50% by volume. The decrease in workability was negligible in mix number ST0.35 and small in ST0.50 which did not need addition HRWR in set A but needed 1 additional ounce in set B to reach the desired slump flow. ST0.65 had a similar slump to ST0.50 but passing ability was greatly reduced and caution must be used when

using 0.65% fiber in small, tight spaces. ST0.80 could not reach the 20” threshold for slump even with 2 extra ounces of HRWR. Although it is possible to reach the desired slump with even higher amounts of HRWR, it would no longer be an economic choice as the rise in cost of the mix would greatly rise.

2. *Mechanical Properties*- As fibers were added in small quantities, the direct tension and compressive strengths decreased compared to the control mix but gained more strength as higher steel fibers amounts were added. The reduction in strength was partially offset with a decrease in modulus, increased ductility and greater restrained shrinkage cracking resistance. ST0.50 and ST0.65 had similar compressive strength to the control mix, with all reaching around 5000 psi at 28 days with one day curing, but were weaker compared to control mix with 7 day curing. ST0.80 showed signs of higher strength, which indicates that very high fiber contents can help to regain loss strength. However, at this high fiber content, workability loss would severely suffer. Tensile splitting results were very similar the compression results with the low fiber mixes being the weakest and the higher fiber contents indicating a regain of strength close to the control mix. The tensile splitting tests did reveal the ductile nature of FRSCC compared to SCC, as the FRSCC samples cracked and flattened instead of cracking and fully splitting apart. Elastic modulus was reduced, up to about 8%, with increasing fiber content. The calculated cracking strain indicated that the control mix had the highest cracking strain at 132 psi, ST0.35 having the lowest with 99 psi and ST0.65 almost matching the control mix at 129 psi.

3. *Free Shrinkage*- The free shrinkage results show that the steel fibers had little effect on shrinkage. ST0.35 had the greatest ultimate shrinkage, most likely due to the

low strength and lower modulus, while all the other mixes including the control mix had very similar ultimate shrinkage (600 microstrain) with one day curing.

4. *Restrained Shrinkage*- From the restrained shrinkage testing, it can be seen that the introduction of fibers does not always delay the first cracking in both ASTM and AASHTO rings. This is most likely due to the decrease in strength and cracking strain. However, the fibers were helpful in preventing small cracks from propagating. In the ASTM rings, the days until fully propagated cracks appeared constantly were longer with additional fiber content despite the rings with fibers initially cracking earlier. In the AASHTO ring, this benefit can be seen by the reduction of large propagated cracks. In ST0.00 and ST0.35, all rings had either full length cracks or cracks at least half the height of the ring. In ST0.50 and ST0.65 only one crack propagated longer than 25% the height of the ring. The largest benefit seen is the decrease in max crack width in both the ASTM and AASHTO rings with fiber. In the ASTM rings, the lowest fiber mix reduced the max crack width by 61% and ST0.50 and ST0.65 reduced crack widths by 73%. In the AASHTO rings, ST0.35 had similar crack widths to the control mix, but ST0.50 was able to reduce max crack widths by 25% and ST0.65 reduced max crack widths by 50%.

5. *Polypropylene Versus Crimped Steel Fiber*- With the same amount of HRWR, the steel fibers maintained a higher flow. All fiber mixes required additional HRWR which the FRSCC mixes in this study only needed additional HRWR for the highest fiber contents. The T20 time and difference in J-Ring flow was better with steel fibers which suggests slightly better workability than PPE fibers. The compressive strength followed a similar trend with both fibers but the PPE fibers increased the tensile splitting strength unlike the steel fiber mixes which had weaker tensile strength. This lead to the FRSCC

mixes with PPE to have higher cracking strain than the control mix. PPE also lead to a small decrease in free shrinkage unlike the steel fibers which saw little affects. In Ghanchi's study, all rings with PPE fibers cracked slightly later than his control mix unlike the steel fiber rings which sometimes cracked earlier. High steel fiber amounts were able to prevent full cracking in the rings better than PPE and the reduction in crack widths were higher with steel fibers.

6. *ASTM Versus AASHTO Rings*- The ASTM ring successfully induced cracks in all the mixes and all rings used. The AASHTO ring setup did not always induce full cracks. The ASTM rings were able to produce cracks around 3 times earlier than their AASHTO ring counterparts and produce crack widths almost 4 times larger. This allows for easier and quicker comparisons. The AASHTO rings, however, can utilize the hexagon VWSG setup used in this study while the ASTM ring is too small to do so.

The FRSCC mix used in this study maintained a good or fair workability up until 0.65% fiber by volume. Steel fibers were shown to reduce the strength and tension, and have little effect on free shrinkage. The steel fibers under restrained conditions did show multiple benefits. The steel fibers do not always prevent cracks from forming, but do delay and sometimes prevent cracking from both propagating and widening. This was shown by a large decrease in crack widths and total cracking area in the restrained shrinkage rings with fibers. The VWSGs, which are not in the standard for the AASHTO ring test, were helpful in picking up when and where cracks are forming. Previous researchers raised concerns that the embedded bolts could sometimes induce cracking, but this study disproves that concern as the distribution of cracks was even and did not favor the area near the bolts.

5.2 Scope for Future Research

This study focused on one type of mix and one type of fiber. Although other research has been done with this mix with PPE fibers, there are other types of fibers that could be utilized including hybrid mixes with multiple fibers. This mix utilized slag but other pozzolans can be used that could be more economical based on the area of the project. Fly ash and metakaolin have been shown to greatly improve shrinkage performance and could be used as a substitute for slag in this mix design. Other admixtures can be used and analyzed for future research. Shrinkage reducing admixtures would help reduce shrinkage but it is currently expensive and large amounts are typically needed. As prices go down, SRAs could become an economic alternative or additive to FRSCC mixes. Viscosity modifying admixtures allow flexibility in SCC mix designs as it can help prevent segregation and bleeding, this allows different mixes to become viable SCC mixes without issues of bleeding. This study used one additional day of wet curing to match more typical field conditions, but a 7 day wet cure of the rings could be more identical to bridge deck curing where FRSCC may become utilized in the near future.

Bibliography

1. T. Wongtanakitcharoen and A. E. Naaman, "Unrestrained early age shrinkage of concrete with polypropylene, PVA, and carbon fibers," *Materials and Structures,* vol. 40, no. 3, pp. 289-300, April 2007.

2. A. Leemann, P. Nygaard and P. Lura, "Impact of admixtures on the plastic shrinkage cracking of self-compacting concrete," *Cement and Concrete Composites,* vol. 46, pp. 1-7, February 2014.

3. E. J. Sellevold and Ø. Bjøntegaard, "Coefficient of thermal expansion of cement paste and concrete: Mechanisms of moisture interaction," *Materials and Structures,* vol. 39, no. 9, pp. 809-815, November 2006.

4. Y. Deng, B. Phares and D. Harrington, "Causes of Early Cracking in Concrete Bridge Decks," *CP Road Map,* pp. 1-6, November 2016.

5. L. Barcelo, M. Moranville and B. Clavaud, "Autogenous shrinkage of concrete: a balance between autogenous swelling and self-desiccation," *Cement and Concrete Research,* vol. 35, no. 1, pp. 177-183, January 2005.

6. E.-i. Tazawa and S. Miyazawa, "Influence of cement and admixture on autogenous shrinkage of cement paste," *Cement and Concrete Research,* vol. 25, no. 2, pp. 281-287, February 1995.

7. N. Jafarifar, K. Pilakoutas and T. Bennett, "Moisture transport and drying shrinkage properties of steel fibre reinforced concrete.," *Construction and building materials,* vol. 73, pp. 41-50, 2014.

8. N. Narayanan and K. Ramamurthy, "Structure and properties of aerated concrete: a review," *Cement & Concrete Composites,* vol. 22, pp. 321-329, April 2000.

9. S. Ahmad, S. K. Adekunle, M. Maslehuddin and A. K. Azad, "Properties of self-consolidating concrete made utilizing alternate mineral fillers," *Construction and Building Materials,* vol. 68, pp. 268-276, 15 October 2014.

10. N. Su, K.-C. Hsu and H.-W. Chai, "A simple mix design method for self-compacting concrete," *Cement and Concrete Research,* vol. 31, no. 12, pp. 1799-1807, December 2001.

11. R. Szecsy, S. Kaufman, D. Henson and T. Abbott, "A modeling approach for the economical, practical production, and placement of SCC for residential and commercial application," *On the Design and Use of Self-Consolidating Concrete,* pp. 187-190, 12 November 2002.

12. T. A. Bier and S. A. Rizwan, "Ecological, Economical and Environmental Aspects of Self Compacting Concrete - Present and Future," *Int. J. Soc. Mater. Eng. Resour.,* vol. 20, no. 1, pp. 12-16, April 2014.

13. O. R. Khaleel, S. A. Al-Mishhadani and H. A. Razak, "The Effect of Coarse Aggregate on Fresh and Hardened Properties of Self-Compacting Concrete (SCC)," *Procedia Engineering,* vol. 14, pp. 805-813, 2011.

14. O. Boukendakdji, S. Kenai, E. H. Kadri and F. Rouis, "Effect of slag on the rheology of fresh self-compacted concrete," *Construction and Building Materials,* vol. 23, no. 7, pp. 2593-2598, July 2009.

15. C. Pumphrey, "How Fluid Concrete Works," InfoSpace Holdings LLC, 2017.

16. B. Felekoglu and H. Sarikahya, "Effect of chemical structure of polycarboxylate-based superplasticizers on workability retention of self-compacting concrete," *Construction and Building Materials,* vol. 22, no. 9, pp. 1971-1980, September 2008.

17. B. Łaźniewska-Piekarczyk, "The influence of selected new generation admixtures on the workability, air-voids parameters and frost-resistance of self compacting concrete," *Construction and Building Materials,* vol. 31, pp. 310-319, June 2012.

18. R. Loser and A. Leemann, "Shrinkage and restrained shrinkage cracking of self-compacting concrete compared to conventionally vibrated concrete," *Materials and Structures,* vol. 42, no. 1, pp. 71-82, January 2009.

19. N. Banthia and J.-F. Trottier, "Concrete Reinforced with Deformed Steel Fibers, Part I: Bond-Slip Mechanisms," *ACI Materials Journal,* pp. 435-446, September-October 1994.

20. R. F. Zollo, "Fiber-reinforced Concrete: an Overview after 30 Years of Development," *Cement and Concrete Composites,* vol. 19, pp. 107-122, November 1995.

21. N. V. Chanh, "Steel Fiber Reinforced Concrete," pp. 108-116.

22. O. Gencel, W. Brostow, T. Datashvili and M. Thedford, "Workability and

Mechanical Performance of Steel Fiber-Reinforced Self-Compacting Concrete with Fly Ash," *Composite Interfaces,* vol. 18, no. 2, pp. 169-294, 2011.

23. S. Grünewald and J. C. Walraven, "Parameter-study on the influence of steel fibers and coarse aggregate content on the fresh properties of self-compacting concrete," *Cement and Concrete Research,* vol. 31, no. 12, pp. 1793-1798, December 2001.

24. V. Corinaldesi and G. Moriconi, "Durable fiber reinforced self-compacting concrete," *Cement and Concrete Research,* vol. 34, no. 2, pp. 249-254, February 2004.

25. M. H. Zhang, C. T. Tam and M. P. Leow, "Effect of water-to-cementitious materials ratio and silica fume on the autogenous shrinkage of concrete," *Cement and Concrete Research,* vol. 33, no. 10, pp. 1687-16944, October 2003.

26. H. Okamura and M. Ouchi, "Self-compacting high performance concrete," *Structural Engineering and Materials,* vol. 1, pp. 378-383, 1998.

27. W. Zhu and J. C. Gibbs, "Use of different limestone and chalk powders in self-compacting concrete," *Cement and Concrete Research,* vol. 35, no. 8, pp. 1457-1462, August 2005.

28. E. Rozière, S. Granger, P. Turcry and A. Loukili, "Influence of paste volume on shrinkage cracking and fracture properties of self-compacting concrete," *Cement and Concrete Composites,* vol. 29, no. 8, pp. 626-636, September 2007.

29. J. M. Khatib, "Performance of self-compacting concrete containing fly ash," *Construction and Building Materials,* vol. 22, no. 9, pp. 1963-1971, September 2008.

30. H. Yazici, "The effect of silica fume and high-volume Class C fly ash on mechanical properties, chloride penetration and freeze–thaw resistance of self-compacting concrete," *Construction and Building Materials,* vol. 22, no. 4, pp. 456-462, April 2008.

31. A. A. Hassan, M. Lachemi and K. M. Hossain, "Effect of metakaolin and silica fume on the durability of self-consolidating concrete," *Cement and Concrete Composites,* vol. 34, no. 6, pp. 801-807, July 2012.

32. E. Güneyisi, M. Gesoglu and E. Özbay, "Strength and drying shrinkage properties of self-compacting concretes incorporating multi-system blended

mineral admixtures," *Construction and Building Materials,* vol. 24, no. 10, pp. 1878-1887, October 2010.

33. Y. Wei, W. Hansen, J. Biernacki and E. Schlangen, "Unified Shrinkage Model for Concrete from Autogenous Shrinkage Test on Paste with and without Ground-Granulated Blast-Furnace Slag," *Aci Materials Journal,* pp. 13-20, January 2011.

34. S. Zhutovsky, K. Kovler and A. Bentur, "Efficiency of lightweight aggregates for internal curing of high strength concrete to eliminate autogenous shrinkage," *Materials and Structures,* vol. 35, no. 2, pp. 97-101, March 2002.

35. H. G. Qin, Z. H. Fei, W. Guo and Q. Tian, "The Effects of Water-Reducer on Early-Age Plastic Shrinkage of Concrete," *Applied Mechanics and Materials,* Vols. 174-177, pp. 1113-1118, May 2012.

36. R. Rodden and D. Lange, “Feasibility of Shrinkage Reducing Admixtures for Concrete,” Center of Excellence for Airport Technology, Urbana, 2004.

37. T. Aly, J. G. Sanjayan and F. Collins, "Effect of polypropylene fibers on shrinkage and cracking of concretes," *Materials and Structures,* December 2008.

38. A. B. Hossain and J. Weiss, "Assessing residual stress development and stress relaxation in restrained concrete ring specimens," *Cement and Concrete Composites,* vol. 26, no. 5, pp. 531-540, July 2004.

39. A. Leemann, P. Lura and R. Loser, "Shrinkage and creep of SCC – The influence of paste volume and binder composition," *Construction and Building Materials,* vol. 25, no. 5, pp. 2283-2289, May 2011.

40. S.-D. Hwang and K. H. Khayat, "Effect of mixture composition on restrained shrinkage cracking of self-consolidating concrete used in repair," *Aci Materials Journal ,* pp. 498-508, September 2008.

41. H. R. Shah and J. Weiss, "Quantifying shrinkage cracking in fiber reinforced concrete using the ring test," *Materials and Structures,* November 2006.

42. A. B. Hossain and J. Weiss, "The role of specimen geometry and boundary conditions on stress development and cracking in the restrained ring test," *Cement and Concrete Research,* vol. 36, no. 1, pp. 189-199, January 2006.

43. Z. Ghanchi, H. Nassif, N. Husam and H. Wang, "Restrained shrinkage behavior of polypropylene fiber reinforced self-consolidating concrete,"

Graduate School - New Brunswick Electronic Theses and Dissertations, 2015.

44. M. C. Brown, C. Ozyildirim and W. L. Duke, "Investigation of Fiber-Reinforced Self-Consolidating Concrete," *Virginia Transportation Research Council*, 2010.